ADVANCED ENERGY MATERIALS
www.advenergymat.de

Programmable Nanocarbon-Based Architectures for Flexible Supercapacitors

Zhiqiang Niu, Lili Liu, Li Zhang, Weiya Zhou, Xiaodong Chen,* and Sishen Xie*

Supercapacitors (SCs), also called electrochemical capacitors, often show high power density, excellent charge/discharge rates, and long cycle life. The recent development of flexible and wearable electronic devices requires that their power sources be sufficiently compact and flexible to match these electronic components. Therefore, flexible SCs have attracted much attention to power current advanced electronics that can be flexible and wearable. In the past several years, many different strategies have been developed to programmably construct different nanocarbon materials into bendable electrode architectures. Furthermore, flexible SC devices with simplified configurations have also been designed based on these nanocarbon-based architectures. Here, recent developments in the programmable assembly of bendable architectures based on nanocarbon materials are presented. Additionally, the design of flexible nanocarbon-based SC devices with various configurations is highlighted. The progress made recently paves the way for further development of nanocarbon architectures and corresponding flexible SC devices. Future development and prospects in this area are also analyzed.

1. Introduction

Supercapacitors (SCs) are one of important energy storage devices due to their higher power density and charge/discharge rates as well as long cycle life.[1–6] In general, a conventional SC is made up of four main components: current collector, electrode material, separator, and electrolyte, as depicted in **Figure 1**a. The recent development of portable, flexible, and wearable electronic devices require SCs to be flexible, simplified, thin, integrated, and high-performance.[7–14] As such, developing flexible SCs with high power and energy densities has attracted significant attention. For a flexible SC, all components, including the electrode material, current collector, separator, electrolyte, and shell, have to have flexibility, even if they are packaged together, as shown in Figure 1b and **Table 1**. In traditional SC devices, the liquid and solid electrolytes and the separators, such as porous polymer film and cellulose fiber paper, are in general flexible. However, conventional carbon-based electrodes are often fabricated by mixing carbon materials with conductive binders and coating these composites onto current collectors. The carbon-based electrodes prepared using this conventional method have poor mechanical properties and cannot endure high strain.[15] In addition, the use of metallic current collectors degrades the gravimetric capacitance of the SC devices and leads to heavy, bulky, or inflexible SC configurations. As a result, conventional SC electrode materials and configurations are not able to meet the requirement of flexible electronic devices.

The two kinds of typical nanocarbon materials, carbon nanotubes (CNTs) and graphene, have fundamental 1D and 2D structures, respectively. They can be used as building blocks for programmable assembly of macroscopic nanocarbon-based structures to directly serve as SC electrodes.[16–25] For a programmable assembly, building blocks should be controllably constructed on the nano-, micro- and macroscale in a time-dependent process, controlling the orientation of components to program the features of nanocarbon-based architectures at different scale levels. As a result, these nanocarbon-based architectures have programmable and tunable features with multiple functions to meet different requirements as flexible SC electrodes, such as good mechanical properties, high electrical conductivity, and controlled porous structure. They are different from the nanocarbon-based architectures with disordered porous structures and degraded performance. The excellent mechanical properties ensure that these programmable nanocarbon architectures can endure the strain and remain original microstructure to great extent during the bending process. Because of the high electrical conductivity, programmable nanocarbon architectures can serve as both electrodes and current collectors, simplifying the SC configuration. Rationally designed porous structures make programmable nanocarbon

Dr. Z. Q. Niu
Key Laboratory of Advanced Energy Materials Chemistry (Ministry of Education)
College of Chemistry
Collaborative Innovation Center of Chemical Science and Engineering
Nankai University
Tianjin 300071, China

Dr. Z. Q. Niu, Dr. L. L. Liu, Dr. L. Zhang, Prof. X. D. Chen
School of Materials Science and Engineering
Nanyang Technological University
50 Nanyang Avenue, Singapore 639798
E-mail: chenxd@ntu.edu.sg

Prof. W. Y. Zhou, Prof. S. S. Xie
Beijing National Laboratory for Condensed Matter Physics
Institute of Physics
Chinese Academy of Sciences
Beijing 100190, China
E-mail: wyzhou@aphy.iphy.ac.cn

DOI: 10.1002/aenm.201500677

architectures act as ideal scaffold to support pseudocapacitive materials, including conductive polymer and transition metal oxides, for further enhancing the overall capacitance of nanocarbon-based electrodes. Furthermore, the morphology, distribution, and orientation of pseudocapacitive materials on the surface of nanocarbon materials are also programmable. Therefore, it is clear that programmable assembly of nanocarbon-based architectures is a promising approach to achieve flexible SC electrodes.

In addition to the fabrication of flexible SC electrodes, the configurations of flexible SC devices should be updated to enhance the flexibility of whole SC device. For instance, unlike liquid electrolyte, gel electrolytes have high mechanical flexibility and integrity as well as desirable electrochemical properties.[26–32] Recent work shows that integrated SC configurations can be achieved using gel electrolyte as both the electrolyte and thinner separator.[26,27,29,33,34] Compared to conventional SC configurations, the novel and simplified SC designs significantly improve the flexibility of SC devices. The salient features of various nanocarbon-based materials and SC devices based on then are summarized in **Table 2**, **3**, **4**, and **5**.

Recently, significant efforts have been made in the programmable assembly of various flexible electrodes based on nanocarbon materials, including CNTs, graphene, and their composites.[35,36] Furthermore, flexible SC devices based on these electrode materials are rationally designed.[8,36–41] Here, we present the recent developments in the programmable assembly of flexible nanocarbon-based architectures and the fabrication of composite electrodes based on nanocarbon materials, conductive polymer, and transition metal oxides. We also describe the diverse design of flexible SCs using these nanocarbon-based architectures as electrodes. The trend to further developments and prospects in this exciting are also analyzed.

2. Pure Nanocarbon-Based Architectures

2.1. CNT-Based Architectures

The classical 1D nanoscale structure of CNTs has attracted much attention for the utilization of CNTs as building blocks to construct different macroscopic structures, such as 2D films and 3D arrays.[16–21] These macroscopic CNT structures can be freestanding or transfer to flexible substrates readily. In addition, they have high specific surface area, excellent conductivity, and good mechanical properties, which are the prerequisites for flexible SC electrodes with high performance. Therefore, because of the successful fabrication of CNT films and 3D arrays, CNT electrodes with high flexibility were significantly more viable. The salient features of pure CNTs-based flexible SC electrodes prepared by various methods are summarized in Table 2.

Vacuum filtration can separate the solid product from a liquid mixture. After vacuum filtrating CNT solution, CNTs can be trapped by the membrane, forming interconnected and entangled CNT films with porous structure.[42–44] If the thickness of CNT films is thick enough, the CNT films can

Zhiqiang Niu is a professor at the College of Chemistry, Nankai University. He received his PhD degree from Institute of Physics, Chinese Academy of Sciences in 2010 under the supervision of Prof. Sishen Xie. After his postdoctoral research in the School of Materials Science and Engineering, Nanyang Technological University (Singapore, supervisor: Prof. Xiaodong Chen), he started his independent research career as Hundred Young Academic Leaders of Nankai University in 2014. His research interests include nanocarbon materials and advanced energy storage devices.

Weiya Zhou is a professor of the Institute of Physics, Chinese Academy of Sciences (CAS). She was graduated from the department of semiconductor of Jilin University in 1984, and received a PhD from Jilin University in 1990. After a postdoctoral research at the University of Groningen (the Netherlands), she joined the Institute of Physics, CAS. She has been engaged in the investigation of carbon nanotubes or the relevant nanomaterials and their characterization as well as their physical properties and possible applications.

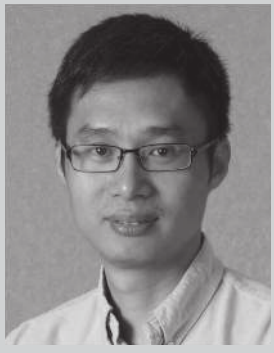

Xiaodong Chen received his BS degree in chemistry from Fuzhou University (China) in 1999, MS degree in physical chemistry from the Chinese Academy of Sciences in 2002, and PhD degree in biochemistry from University of Muenster (Germany) in 2006. After working as a postdoctoral fellow at Northwestern University (USA), he started his independent research career as a Singapore National Research Foundation Fellow and Nanyang Assistant Professor at Nanyang Technological University in 2009. He was promoted to Associate Professor with tenure in September of 2013. His research interests include interactive materials and devices, programmable materials for energy conversion, and integrated nano-biointerface.

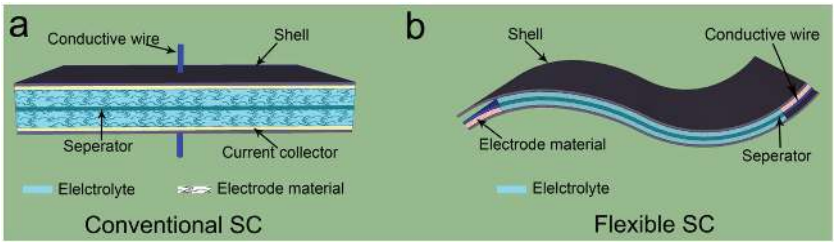

Figure 1. Schematic diagrams of a) conventional and b) flexible SCs.

be peeled off from membrane as freestanding films.[45] CNT film electrodes obtained by vacuum filtration possess uniform thicknesses as well as high mechanical strength. Thus they can serve as a flexible SC electrode. However, their area is difficult to scale up.

Recently, freestanding single-walled CNT (SWCNT) films that have a continuous reticulate architecture (**Figure 2**a) were obtained using a floating catalyst chemical vapor deposition (FCCVD) technique.[15,20,46] Because of the continuous reticulate structure, these directly synthesized SWCNT films display higher electrical conductivity (about 2000 S cm^{-1}) and mechanical properties than the case of post-deposited SWCNT films. Such SWCNT films are able to be spread out onto the separators (Figure 2b) to serve as both electrodes and current collectors for a SC device in compact design (Figure 2c).[15] Furthermore, the thickness and transparency of directly grown SWCNT films can be improved by a "repeated halving" approach, obtaining ultrathin, transparent, and conductive films.[47] SWCNT films can endure large strain and remain stable conductivity because of several possible current pathways even when some links are disconnected.[7,48,49] However, when large strain (>10%) is applied to the SWCNT films, the electrical conductivity of films will be decreased seriously. To enhance their stretchability, SWCNT films with buckled structures were fabricated.[50] Based on buckled SWCNT films on PDMS, stretchable SCs were assembled and the stretchability of these SCs can reach about 30%.[50] Continuous reticulate structure results in higher strain tolerance of directly synthesized SWCNT films in comparison with the case of post-deposited SWCNT films. By combining directly grown SWCNT films with the prestrained polydimethylsiloxane (PDMS), buckled SWCNT films with 140% stretchability can be fabricated (Figure 2d).[51] Utilizing such buckled SWCNT films as electrodes, highly stretchable integrated SWCNT film SCs were obtained based on polyvinyl alcohol (PVA)/H_2SO_4 gel electrolyte, as shown in Figure 2e. The resulting integrated SCs were able to be stretched as an integrated unit, which overcame the limitation of conventional stretchable SCs wherein both electrodes in general move relative to separator during the stretching process. The performance of as-prepared stretchable SCs is nearly unchanged at 120% strain and even in the stretching process. Although the directly grown SWCNT films possess high conductivity and mechanical properties, their thickness is thin and limited (in general <1 μm). Furthermore, they have high surface energy, leading to strong self-adhesion. As a result, it is difficult to directly use or spread out them onto various substrates to serve as SC electrodes.

Based on other solution-based methods, SWCNT films can be deposited onto various flexible plastic substrates (Table 2). The substrate-supported SWCNT films would be also promising candidates of flexible SC electrodes. For example, using a spray coating technology, flexible SWCNT film electrodes were prepared on polyethylene-therephthalate (PET) substrate (Figure 2f).[7] The high conductivity and excellent mechanical properties of the SWCNT networks assist the fabrication of flexible SC devices (Figure 2g). To make the SCs more flexible and printable, polymer gel was served as electrolyte and separator. The SCs based on gel electrolyte have a specific capacitance of about 110 F g^{-1}, which is comparable to the case in aqueous electrolyte.

Unlike plastic substrates, which have a flat surface, porous paper and textiles exhibit a set of properties due to their flexibility and inherent porosity. For instance, there are a large number of functional groups on the surface of cellulose fiber (CF) in the paper, which is helpful for binding additive functional materials. In addition, the porous structure is able to improve the fast mass and electron transport kinetics.[52–57] Therefore, paper is a good scaffold to support other functional

Table 1. Comparison of conventional and flexible SCs.

	Conventional SC	Flexible SC
Requirement for Electrode materials	High SSA, conductive	Thin, lightweight, flexible, High SSA, high conductive
Electrode materials	AC, CNT, graphene, GO derivatives, conductive polymer, transition metal oxide	Films or fibers based CNT or/and graphene (rGO), Hybrid films or fibers using CNT or/and graphene (rGO) as skeleton to deposit conductive polymer and transition metal oxide
Coductive Binder	PVDF,PTFE, etc.	None
Currrent collector	Ni foil foam, stainless steel foil, etc.	None
separator	Porous polymeric films, woven glass fibers, porous woven ceramic fibres	Solid state or gel polymer and salt electrolyte, filter paper, porous polymeric films
Electrolyte	Aqueous electrolyte	Solid state or gel polymer and salt electrolyte
	Organic electrolyte	Aqueous electrolyte
		Organic electrolyte
Seal materials	Coil type, stainless steel, platic etc.	None or plastic film

Table 2. Summary of various flexible CNT electrodes.

Electrode materials	Method	Substrate	Electrolyte	Specific capacitance [F g^{-1}]	Energy density [W h kg^{-1}]	Power density [kWkg^{-1}]	Ref.
MWCNT film	Vacuum filtration	Freestanding	38 wt% H_2SO_4	104[b]	–	8	[45]
MWCNT array	CVD	Cellulose	Ionic liquid/Cellulose	22[b]	13	1.5	[63]
MWCNT sponge	CVD	Freestanding	1 M $LiPF_6$	28.5[b]	–	–	[64]
DWCNT film[a]	Vacuum filtration Heat-treatment	Freestanding	38 wt% H_2SO_4	66.9[c]	–	–	[44]
SWCNT film	Spray coating	PET	PVA/H_3PO_4	110[b]	6	23	[7]
SWCNT film	Meyer rod coating	Paper	1 M H_2SO_4 1 M $LiPF_6$	200[b]	30–47	200	[58]
SWCNT film	Drop-dried	Paper	Ionic-liquid-based gel	135[b]	41	164	[34]
SWCNT film	Dipping an drying	Textile	1 M $LiPF_6$	0.48 F cm^{-2}[b]	20	10	[59]
SWCNT film	Dipping an drying	Textile	PVA/H_3PO_4	115[b]	49	–	[60]
SWCNT film	FCCVD	Freestanding	1 M $LiClO_4$ PVA/H_2SO_4 1 M $C_8H_{20}BF_4N$	35–55[b]	43 ($LiClO_4$)	197($LiClO_4$) 32(PVA/H_2SO_4)	[15,50,51]
SWCNT film	Repeated halving	PET	1 M $LiClO_4$	22.5[b]	12.5	13.9	[47]
SWCNT fiber	Spray coating, Wrapping, Dipping an drying	Rubber fiber, CF, carbon fiber	PVA/H_3PO_4	10–20[b]	–	–	[70–72]

[a]Phosphorus-enriched carbon, [b]two-electrode, [c]three-electrode.

materials to achieve lightweight and flexible composite paper electrodes. SWCNT films can be coated onto CF paper by a simple solution process. The sheet resistance of the SWCNTs-coating composite paper is about 1 Ω sq^{-1}.[58] The SCs based on SWCNT-coating paper display excellent electrochemical performance, as shown in Table 2. In order to enhance the flexibility of SCs, all-solid-state SCs based on CNT/CF composite paper can be designed by using an gel electrolyte.[34] The

Table 3. Summary of various flexible graphene-based electrodes.

Electrode materials	Method	Substrate	Electrolyte	Specific capacitance [F g^{-1}]	Energy density [Whkg^{-1}]	Power density [kWkg^{-1}]	Ref.
rGO foam	Leavening	Freestanding	1 M H_2SO_4	110[d]	–	–	[91]
rGO film	Vacuum filtration	Freestanding	1 M H_2SO_4	215[d]	–	414	[83]
rGO film	Vacuum filtration	PET	2 M KCl	111[e]	15.4	0.554	[86]
rGO film[a]	Vacuum filtration	Freestanding	$TEABF_4$/AN	120[d]	26	500	[84]
rGO film	Vacuum filtration	Paper	PVA/H_2SO_4	7.6 mF cm^{-2}[d]	—	—	[105]
rGO film	Vacuum filtration	polyurethane	1 M H_2SO_4	156[e]	—	—	[85]
rGO foam	Vacuum filtration/ Template assemble	Freestanding	6 M KOH	58[e]	30–47	200	[88]
rGO film	Laser irradiation	GO paper	H_2O	0.51 mF cm^{-2}[d]	0.43 mWh cm^{-3}	1.7 W cm^{-3}	[95]
rGO foam	Laser irradiation	Freestanding	PVA/H_3PO_4	3.67 F cm^{-2}[d]	1.36 mWh cm^{-3}	20 W cm^{-3}	[93]
rGO film[b]	LBL	Freestanding	6M KOH	80	—	—	[90]
rGO film[b]	Electrophoresis	PET	1 M LiClO4	65[d]	36	49	[89]
rGO film[c]	Vacuum filtration	Freestanding	6M KOH	138[d]	—	—	[87]
rGO film	Brush coating and drying	Cotton cloth	6M KOH	81.7[d]	7.13	1.5	[107]
rGO film	Paper-making,Hydrotherma 1 dipping-drying	Cellulose paper	1 M$LiPF_6$ PVA/ H_2SO_4	191[d] 464[e]	153	2.4	[104,106]
rGO fiber	Hydrothermal and electrlyzing	Freestanding	PVA/H_2SO_4	25–40[d]	0.4–1.7 × 10^{-4} mWh cm^{-2}	6–100 × 10^{-6} cm^{-2}	[112]
CNT/rGO film	Vacuum filtration	Freestanding/PET	1 M KC1, 6M KOH	150–400[e]	—	—	[117–119]
CNT/rGO fiber	Hydrothermal	Freestanding	PVA/H_3PO_4	45 F cm^{-3}[d]	1–10 mWh cm^{-3}	0.01–1 W cm^{-3}	[125]
CNT/rGO film	LBL	Flexible substrate	1 M H_2SO_4	120[e]	—	—	[121]

[a]Activated by KOH, [b]separated by Au NP, [c]separated by CB NP, [d]two-electrode, [e]three-electrode.

Table 4. Summary of various flexible nanocarbon and conductive polymer hybrid electrodes.

Electrode materials	Method	Substrate	Electrolyte	Specific capacitance [F g^{-1}]	Energy density [Whkg^{-1}]	Power density [kWkg^{-1}]	Ref.
SWCNT/PANI	Eectro-deposition	Freestanding	1 M $LiClO_4$	236[a)]	131	62.5	[152]
MWCNT /PANI	Chemical Polymerization	Freestanding	1 M H_2SO_4	424[a)]	–	–	[132]
MWCNT /PANI	Polymerization	Freestanding	PVA/H_2SO_4	350[a)]	7.1	2.189	[29]
SWCNT/PANI	chemical polymerization	Cloth	1 M H_2SO_4	410[a)]	26.6	7	[154]
SWCNT/PANI	Painting	PVA/H_3PO_4	PVA/H_3PO_4	16[a)]	0.5	0.3	[148]
SWCNT /PANI	Electrochemical polymerization	PET	1 M H_2SO_4	55[a)]	–	–	[136]
SWCNT/PEDOT	Vacuum filtration	Freestanding	1 M $NaNO_3$	104[a)]	7	0.825	[155]
rGO/PANI-NF	Vacuum filtration	Freestanding	1 M H_2SO_4	210/301[a)]	15–19	0.1–10	[147]
rGO/PANI	LBL	Flexible substrate	1 M H_2SO_4	400[b)]	30	1	[165]
rGO/PANI rGO/PPy	Electro-polymerization	Freestanding	1 M H_2SO_4	233[b)]			[167]
	LBL	Flexible substrate	1 M NaCl	165[a)]			[172]
rGO/PPy	Pulse-Electro-polymerization	Freestanding	1 M KCl	237[a)]	33	1.18	[169]
CNT/RGO/PPy	Vacuum filtration	Freestanding	1 M KCl	211[b)]	–	–	[174]

[a)]two-electrode, [b)]three-electrode.

resultant all-solid-state SC can be repeatedly bent and there is no significant variation in their electrochemical properties. Like SWCNT-coating papers, conductive textile can be prepared by a simple "dipping and drying" process based on SWCNT ink, as shown in Figure 2h,i.[59,60] Compared with directly grown CNT films, the substrate-supported CNT films based on

Table 5. Summary of various flexible nanocarbon and transition metal oxide hybrid electrodes.

Electrode materials	Method	Substrate	Electrolyte	Specific capacitance [F g^{-1}]	Energy density [Whkg^{-1}]	Power density [kW kg^{-1}]	Ref.
CNT/MnO_x	ED	Freestanding	0.1 M Na_2SO_4	<1250 [b)]	49–135	1–17.4	[176]
SWCNT/MnO_2	Redox reaction	Freestanding	1.0 M Na_2SO_4	529.8[a)]	73.6	14.6	[105]
SWCNT/MnO_2	Redox reaction	Cloth	2 M Li_2SO_4	0.41 Fcm^{-2}[a)]			[59]
SWCNT/MnO_2	ED	Textile	0.5 M Na_2SO_4	2.8 Fcm^{-2}[b)]	5–20	13	[178]
SWCNT/MnO_2	ED	Sponge	1 M Na_2SO_4	1230[a)]	31	63	[179]
SWCNT/MnO_2	ED	Paper	0.1 M Na_2SO_4	540[b)]	20	1.5	[180]
CNT/MnO_2	ED	Carbon fabric	1 M Na_2SO_4	740[b)]	–	–	[177]
SWCNT/RuO_2	Dip-coating	Flexible substrates/ Cloth	PVA/H_3PO_4	138[a)]	18.8	96	[182]
SWCNT/In_2O_3	Dip-coating	PET	1 M $LiClO_4$	64[a)]	1.29	7.48	[181]
SWCNT/RuO_2/ In_2O_3	Dip-coating	Freestanding	1 M Na_2SO_4	184[c)]	25.5	50.3	[183]
CNT/V_2O_5	ALD	Flexible substrate	8 M LiCl	600[a)]	–	–	[185]
CNT/TiO_2	Pulse-Electro-Polymerization	Freestanding	1 M H_2SO_4	36.8[a)]	–	–	[186]
rGO/MnO_2	ED	Freestanding	1 M Na_2SO_4	389[c)]	44	25	[191]
rGO/MnO_2	Vacuum filtration	Freestanding	0.1 M Na_2SO_4	256[b)]	–	–	[188]
rGO/MnO_2/ PEDOT:P SS	ED	Textile	0.5 M Na_2SO_4	380[b)]	–	–	[194]
rGO/MnO_2	ED	Textile	0.5 M Na_2SO_4	315[c)]	12.5	110	[193]
rGO/ZnO	Chemical syntheses	PET	1 M KCl	51.6[b)]	–	–	[198]
rGO/Co-Al LED	LBL	Flexible substrate	1 M KOH	1200[b)]	–	–	[212]
CNT/rGO/Co_3O_4	Hydrothermal method	Freestanding	3M KOH	378[b)]	–	–	[202]
CNT/rGO/MnO_2	Chemical coprecipitation	Freestanding	1 M Na_2SO_4	372[b)]	2.2	42	[228]

[a)]two-electrode, [b)]three-electrode, [c)]asymmetric SCs, ED: Electrodeposition.

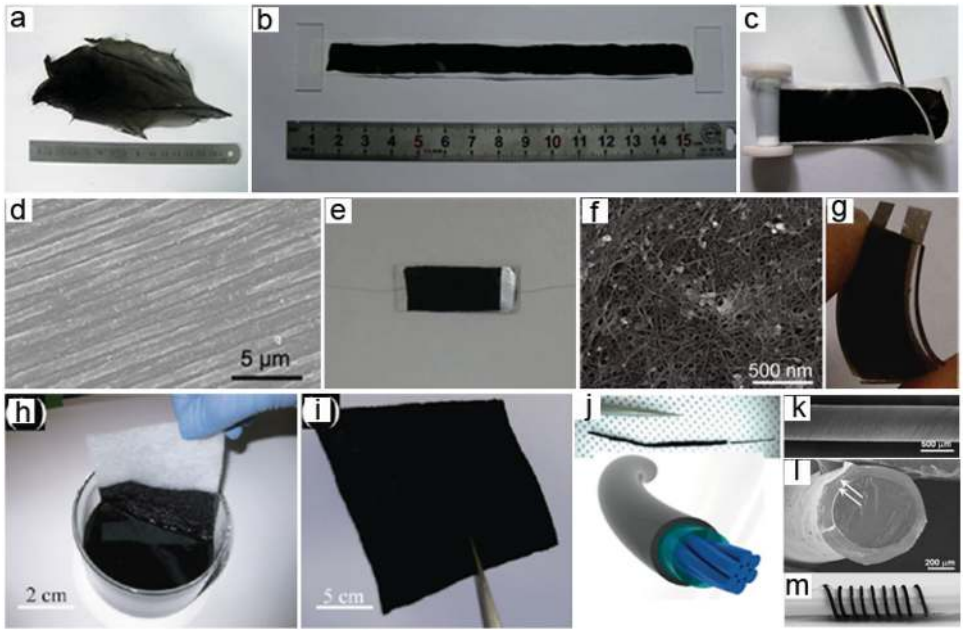

Figure 2. Optical images of a) the directly grown SWCNT film by FCCVD, b) the directly grown SWCNT films on the separator, and c) rolled two separators with SWNCT films. Reproduced with permission.[15] Copyright 2011, Royal Society of Chemistry. (d) SEM image of buckled SWCNT film on PDMS substrate. e) Optical image of a stretchable SC with integrated configuration using buckled SWCNT films as electrodes. Reproduced with permission.[51] f) Scanning electron microscopy (SEM) image of SWCNT films obtained by spray coating. g) Optical image of SC device using sprayed SWCNT films on PET and PVA/H_3PO_4 as electrodes and electrolyte, respectively. Reproduced with permission.[7] Copyright 2009, American Chemical Society. h) Conductive SWCNT-coating textiles are fabricated by a "dipping–drying" process. i) A conductive SWCNT-coating textiles with 10 cm × 10 cm size. Reproduced with permission.[59] Copyright 2010, American Chemical Society. j) Schematic and digital photo of a coaxial fiber SC. Reproduced with permission.[56] k) SEM and l) cross-section SEM image of a fiber SC. m) Photograph of a fiber SC being wound on a substrate. Reproduced with permission.[72]

solution-based methods are easy to scale up. However, the use of substrates would increase the weight of entire SC device.

In addition to CNT films, CNT arrays and sponges are also the good candidates of flexible SC electrodes.[61–64] By combining a CNT array and cellulose with ionic liquid, different components of SC, including electrodes, separator, and electrolyte were integrated into one single integrated unit, which was able to be used as a building block for flexible energy storage devices with thin thicknesses.[63] The SCs based on such a composite show a specific capacitance of 22 F g^{-1} and a power density of 1.5 kW kg^{-1}. CNT sponges with appropriate thickness synthesized by CVD can also be compressed into thin films by a mechanical instrument or hydraulic punching to act as flexible SC electrodes.[64] Because CNT arrays and sponges often grow on the surface of inflexible substrates, they have to be transferred to flexible substrate to serve as SC electrode. Furthermore, as with directly grown CNT films, the preparation of CNT arrays and sponges is also difficult to scale up.

Because of the unique structure of CNTs, CNTs are able to be constructed into fibers using single CNT or bundle as building blocks.[21,65–68] The CNT fibers can be used in composite materials due to their high strength.[21,36,46,69] However, the CNT fibers cannot directly act as high-performance fiber SC electrodes because electrolyte ions cannot diffuse into the compact structure of the CNT fibers deeply. To overcome this issue, the CNTs are often coated onto the surface of fiber substrate, such as rubber fiber, carbon microfibers and natural CF (Figure 2j) to serve as fiberSC electrodes.[70–72] For instance, the aligned CNT sheets can sequentially wrap on an elastic fiber to use as two electrodes, forming coaxial fiberSC (Figure 2k–m).[72] The specific capacitance of fiber SCs still can be about 18 F g^{-1} after stretching 75% for 100 cycles.

2.2. Graphene-Based Architectures

The theoretical specific surface area and Young's modulus of graphene are 2630 m^2 g^{-1} and ~1.0 TPa, respectively.[73,74] In addition, graphene displays good electrical conductivity.[75] Clearly, graphene is promising for an electrical double layer capacitor (EDLC) electrodes and support for active pseudocapacitive materials.[35] Graphene sheets and its derivatives are able be acted as basic building blocks to programmably construct macroscopic graphene structures.[22–24] However, different from CNTs, graphene sheets tend to restack during the assembling process due to the strong π–π stacking and van der Waals force between graphene sheets. As a result, the unique ultrahigh surface area of graphene sheets would be lost. Therefore, preventing the aggregation of graphene sheets in paper-like films is key to constructing flexible graphene SC electrodes. To avoid the self-aggregation of graphene sheets, various strategies have been developed to fabricate graphene porous structures for flexible SC electrodes, as shown in Table 3.

Large-scale production of graphene sheets with controlled layers, size, morphology, and chemical properties is the first step to construct macroscopic programmable graphene

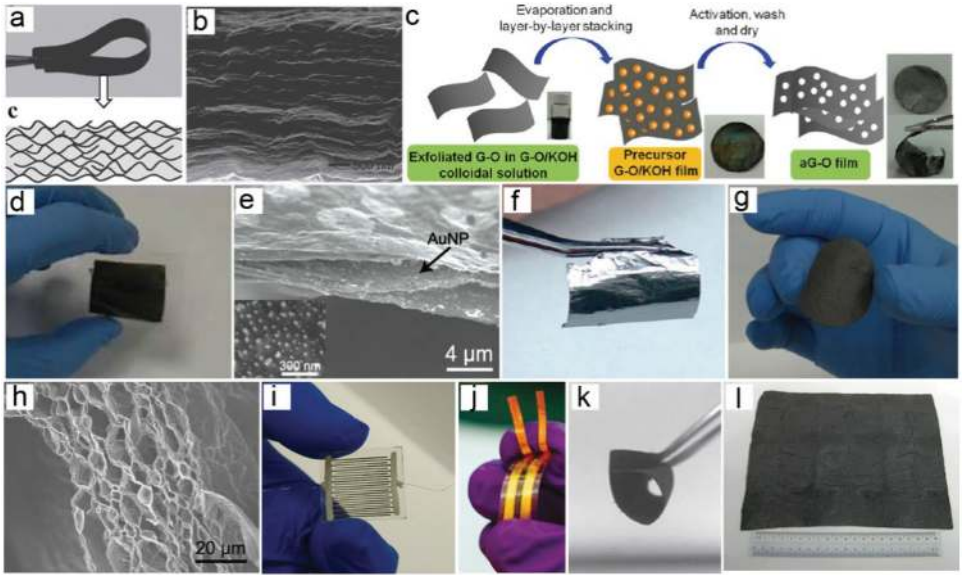

Figure 3. a) Optical and b) SEM images of a self-stacked, solvated rGO film. Reproduced with permission.[83] c) The experimental steps of activated rGO film. Reproduced with permission.[84] Copyright 2012, American Chemical Society. d) Optical and e) SEM images of rGO/AuNP composite film on PET. Reproduced with permission.[89] f) Optical images of multilayered rGO film with different size rGO sheets. Reproduced with permission.[90] Copyright 2010, American Chemical Society. g) Optical and h) cross-sectional SEM images of rGO foam achieved using a leavening process. Reproduced with permission.[91] i) Optical image of rGO micro-SCs on PET. Reproduced with permission.[96] (j) flexible in-plane micro-SC device based on pristine graphene. Reproduced with permission.[103] Copyright 2011, American Chemical Society. k) rGO/paper composite film obtained using vacuum filtration. Reproduced with permission.[105] l) rGO/paper composite film obtained by combining "dipping and drying" and hydrothermal processes. Reproduced with permission.[106]

films.[22,76] Solution-phase exfoliation of graphite is a promising technology to produce graphene and its derivatives, such as graphene oxide (GO).[22,77–81] GO sheet is an electrical insulator because of its disrupted sp^2 bonding networks, but its conductivity can be recovered by restoring the π-network.[80] Therefore, GO usually acts as the precursor of graphene to rationally construct programmable graphene architectures.

The reduced graphene oxide (rGO) films formed by vacuum filtration usually have a compact structure due to the shearing field-assisted alignment of rGO sheets during vacuum filtration process.[82] However, if the rGO films are not fully dried, the rGO sheets will be largely separated by a solvated state (**Figure 3**a,b), which leads to a highly porous structure. Such a porous structure allows the electrolyte ions to easily access the surface of individual rGO sheets, resulting in ultrahigh power density and high energy density.[83] Furthermore, rGO sheets can be activated by KOH, forming porous rGO sheets. By vacuum filtering porous GO sheets decorated with KOH, highly conductive and flexible porous rGO thin films can be obtained, followed by an activation step, as shown in Figure 3c.[84] The thickness of such rGO films is able to be controlled by the volume and the concentration of the solution during the vacuum filtration process.[85] The rGO film with 25 nm thickness can be obtained by vacuum filtering for flexible and transparent SC electrodes.[86]

Adding a "spacer" to the inner rGO film is another approach to avoid the aggregation of rGO sheets in the films. By direct vacuum filtrating the mixed solution of rGO and other nanomaterials, flexible paper electrodes with porous rGO-based structure would form.[87,88] The mediated pores in as-prepared rGO films enhance the diffusion of electrolyte into the inner of films, which is of significance for high rate SC electrodes. The addition of a spacer in the rGO films can also be realized by other methods, such as electrophoretic alternate deposition and LBL self-assembly, forming multilayered structures. Using Au nanoparticles (NPs) as a spacer, alternately multilayered rGO/Au NP films were fabricated by electrophoretic alternate deposition, as shown in Figure 3d,e.[89] LBL self-assembly is another way to prepare multilayered rGO-based films by alternately assembling rGO sheets and other nanomaterials onto different substrates. Freestanding and flexible multilayered films with variable sized graphene sheets can be prepared by LBL assembly based on capillary force driven (Figure 3f).[90] Although the addition of a spacer can effectively prevent the aggregation of graphene sheets in rGO films, their process is complicated and the addition of a spacer usually degrades the conductivity of the resultant films.

Leavening is a process of transferring compact dough to porous structures during baking or steaming. Inspired by this, the paper-like rGO foams with continuous porous cross-linked structures were fabricated by a similar leavening process (Figure 3g).[91] The resultant rGO foams effectively avoid the re-stacking between rGO sheets. Furthermore, there are better conductive contacts between the sheets in the foam due to the continuous cross-linked structure (Figure 3h), leading to low resistance of foams (less than 100 Ω sq^{-1}). Additionally, 3D rGO foams can be transfered to films with porous structures by physical methods to serve as flexible SC electrodes.[92] Laser irradiation of the GO film can induce the reduction of GO into rGO to improve electrical conductivity and obtain porous structures. Based on the direct laser reduction of GO films, flexible rGO films with an open network and microscale rGO electrodes were prepared.[93–95] The as-prepared porous rGO films show excellent mechanical properties,

high electrical conductivity of 1738 S m^{-1}, and a specific surface area of 1520 m^3 g^{-1}.[93] The rGO films achieved by leavening and laser irradiation exhibit larger pore size than the case produced by vacuum filtering, leading to better diffusion of the electrolyte in their pores. The rGO films obtained by vacuum filtering possess high power density due to their high conductivity.

Miniaturizing SC devices onto a chip can remove intricate interconnections in bulk-sized SC devices to effectively increase the density of SC devices and reduce their design complexity on one chip. Furthermore, microscale SC units are of great significance for integrating SC devices with other electronic circuits to design a self-powered device system. In order to fabricate a micro-SC, a microelectrode structure has to be designed on a substrate. Graphene nanosheets are significantly suited to assemble micro-SC electrode pattern because of their unique structure and excellent properties. Lateral rGO interdigitated microelectrodes with thin thickness can be fabricated by combining photolithography with selective electrophoretic buildup or selective wetting.[96–98] Based on these micro-electrodes, all-solid-state micro-SCs with high flexibility were fabricated by coating PVA/H_3PO_4 gel electrolyte onto these microelectrodes, as shown in Figure 3i.[96] Combining photolithography with inkjet printing or spin coating, graphene-based in-plane micro-SCs can also fabricated.[99–102] Unfortunately, these micro-SC devices were designed on inflexible substrates. If the inflexible substrates are replaced by bendable substitute, the flexibility of the micro-SC devices will be improved significantly. In addition to rGO film obtained from GO, pristine graphene can serve as the electrodes of in-plane ultrathin micro-SCs (Figure 3j).[103] Although high gravimetric energy and power densities are often achieved for micro-SCs with thin thickness, their areal energy density is limited since the mass of the active electrode materials is often a small fraction of the total mass of the SC device.

Graphene sheets coated CF composite papers are able to be prepared by a simple paper-making process.[104] However, in such composite paper, the graphene sheets are only coated on the CF surface and the pores of paper cannot effectively used. Although rGO nanosheets can directly fill into the pores of filtering paper by vacuum filtration (Figure 3k),[105] they are randomly oriented and seriously aggregated. In order to fully utilize the CF surface and the pores in paper, a thin GO layer was first coated onto the CF surface in the paper by a simple "dipping and drying" strategy and then microscale porous rGO architectures were assembled into the pores of paper using a hydrothermal process, forming nanostructured rGO/CF composite paper (Figure 3l).[106] The nanostructured architectures in rGO composite paper effectively overcome the aggregation of rGO sheets to improve the penetration of liquid ions and are beneficial for transporting the electrons throughout the CF network. Furthermore, rGO/CF composite paper can be used as a scaffold to support polyaniline (PANI). After depositing PANI, their tensile strength and Young's modulus are enhanced. In addition to CF paper, cotton cloth has been used to support rGO to fabricate flexible rGO electrode by a "brush coating-drying-annealing" method.[107]

Because of the irregular size and shape of graphene sheets, it is a challenge to construct graphene sheets into fiber structures. Currently, a variety of strategies have been developed to assemble graphene-based fibers.[108–116] For instance, rGO fibers that have a density of 0.23 g cm^{-3} can be obtained by a dimensionally confined hydrothermal strategy.[108] Such rGO fibers were able to serve as a substrate to support a layer of porous graphene network, which can be used as the electrodes of flexible all-solid-state fiber SC.[112] The resulting fiber SC shows excellent flexibility that is similar to the single rGO fiber. Therefore, all-solid-state fiber SCs are able to be woven into a textile to match the wearable electronics.

2.3. CNTs-Graphene Composite Architectures

As mentioned in Section 2.1 and 2.2, the SC electrodes based on CNTs often provide high power density because of the high conductivity of CNTs. The rGO-based SC electrodes usually show high specific capacitance that is ascribed to the high specific surface area of rGO sheets. If CNTs and rGO sheets are combined together, it will be a compromise between the excellent conductivity from CNTs and the large specific surface area from rGO. Flexible MWCNT/rGO hybrid films that possess an interconnected network as well as a double-layer structure are able to be fabricated by vacuum-filtration, followed by transferring to flexible substrate and reducing GO to rGO, as shown in **Figure 4**a.[117] The MWCNT/rGO hybrid films are transparent

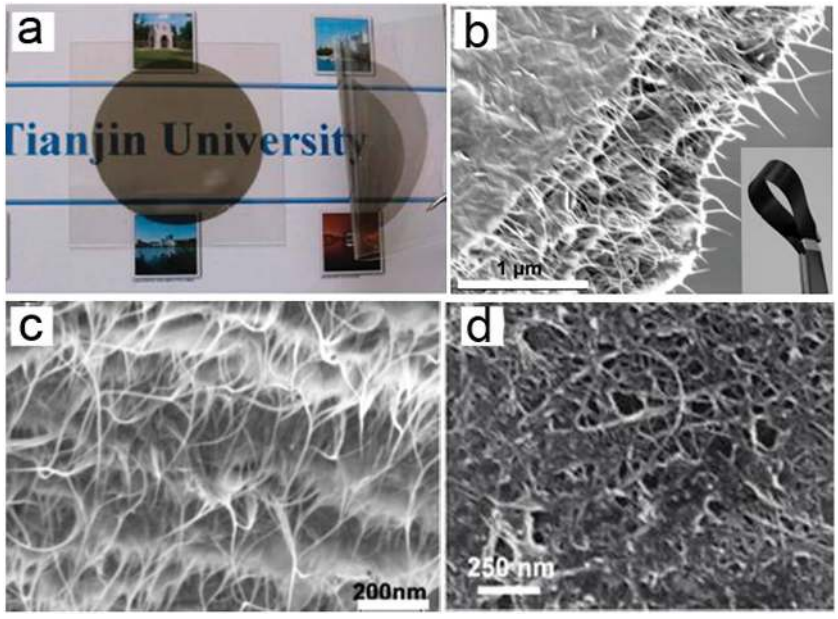

Figure 4. a) MWCNT/rGO hybrid electrode on a PET sheet. Reproduced with permission.[117] Copyright 2012, American Chemical Society. b,c) SEM images of the freestanding rGO/CNT hybrid film. Reproduced with permission.[120] d) SEM image of the [poly(ethyleneimine)-GN/MWNT-COOH]$_9$ film after nine deposition cycles. Reproduced with permission.[121] Copyright 2010, American Chemical Society.

and highly conductive. If the thickness of rGO/CNT composite films was increased, freestanding rGO/CNT films can be fabricated (Figure 4b,c).[118–120] Stable CNT aqueous solution can be obtained by charge stabilization from acid oxidation that can result in negative charges on the surface of the CNTs. Positively charged polymer-modified GO dispersions are able to be achieved by in situ reduction of GO sheets in the presence of cationic poly(ethyleneimine).[121] The positively charged poly(ethyleneimine)-modified rGO sheets and negatively charged acid-oxidized MWCNTs were co-assembled into multilayered rGO/CNT hybrid films, which possess interconnected carbon structures with well-defined nanoscale pores(Figure 4d).

The performance of graphene-based SC materials is often limited due to the aggregation and restacking of graphene, and the actual accessible surface area of the graphene-based electrodes is much lower in comparison with the theoretical surface area. The addition of spacers and the in-plane design of SC micro-electrodes can be used to avoid this problem. If these two methods are used together, high-performance micro-SCs will be obtained. Based on this mechanism, interdigital electrodes of rGO and CNT composites can also be fabricated by combining photolithography and electrostatic spray deposition or CVD.[122,123] However, these micro-SC based rGO/CNT composite is inflexible due to the limit of substrate. To obtain flexible rGO/CNT micro-SCs, the interdigital electrodes of rGO and CNT composites were achieved on the flexible plastic substrate by laser irradiation of GO and CNT composite film.[124] In the presence of CNTs with a smaller diameter, the laser-scribed rGO/CNT micro-SC was found to yield the better energy storage performance.

Because neat rGO fibers often have compact structure, they cannot be directly used as fiber SC electrodes. To overcome this issue, hierarchically nanostructured carbon microfibers that are made of a SWCNTs/nitrogen-doped rGO sheet interconnected network architecture were fabricated using a scalable hydrothermal synthesis. The resultant hybrid fibers exhibit excellent electrical conductivity and large accessible surface area, indicating they are good candidate of fiber SC and self-powered nanosystem electrodes.[125,126]

Pure CNTs- and/or rGO-based SCs are EDLCs and this depends on their specific surface area and electrical conductivity. For flexible CNTs- and/or rGO-based SC electrodes, good mechanical properties, namely, the ability to endure the strain originated from bending, is another important factor that has to be considered. Flexible CNTs- and/or rGO-based SC electrodes can be divided into two categories: freestanding and substrate supported films. Freestanding films provide us with the opportunity to tailor them into desired shapes for electrode material to match the requirements for flexible SC devices. Good strength and toughness allow the freestanding films to maintain its structure and integrity in bending, even rolling processes. As mentioned above, freestanding CNT films were often prepared by CVD and vacuum filtration. Therefore it is difficult to scale up their area. Compared to post-deposited CNT films obtained by vacuum filtration, the SWCNT films directly grown by CVD have better electrical conductivity and mechanical properties. As a result, they can serve as stretchable SC electrodes. However, the directly grown SWCNT films display strong self-adhesion because of their high surface energy and large surface-to-volume ratio, thus it is difficult to handle them. Different from CNTs, the strong π–π stacking and van der Waals force between graphene sheets tend to lead to the self-agglomeration of graphene sheets during the process of preparing graphene films. As a result, the unique ultrahigh surface area of the graphene sheets was lost. Post-treatment or addition of a spacer is often used to overcome this problem, resulting in a complicated process.

Different from freestanding film electrodes, the production of substrate supported CNT or graphene films can be done on a large scale. Substrate supported CNT or graphene films can be achieved by assembling CNTs or graphene onto various substrates, such as plastic, CF paper, and cloth. The uniform assembly of CNT or graphene onto the substrate surface is the key step of obtaining substrate supported CNT or graphene films with high performance. For the plastic substrate with flat surface, they often serve as both the support of CNT films and shell of devices. However, the flexibility of the plastic substrate is not good enough, limiting the flexibility of whole SC device. Because of the self-agglomeration between rGO, the pure rGO films on plastic substrates show low performance in general. To improve their performance, a "spacer" has to be added to the films or the films are patterned into interdigitated microelectrodes. Compared to plastic substrates, paper and cloth have better flexibility. Furthermore, they possess porous structure and large specific surface area, leading to high CNT or graphene loading and good accessibility of electrolyte.

The high electrical conductivity of pure CNTs and graphene electrodes endow them with high power density. However, pure CNTs- and/or rGO-based electrodes often suffer from a major problem that not all their Brunauer-Emmett-Teller (BET) surface area is electrochemically accessible in actual SC application.[127] Therefore, their energy densities are relatively low, as shown in Table 2 and 3. The enhancement of their energy density should be considered.

3. Nanocarbon/Conductive Polymer Composite Architectures

The pseudo-capacitance that is ascribed to the faradic or redox reactions of electroactive materials often shows high energy density. Therefore, pseudo-capacitance is often combined with the EDLC to improve the overall capacitance of SC electrode materials. Conductive polymer and transition metal oxides are the main electrochemical materials with pseudo-capacitance and they have been widely studied in SCs. To enhance the energy density of pure CNTs and graphene electrode materials, much effort has gone by combining the pseudo-capacitance from conductive polymer and transition metal oxides with the EDLC of CNTs and graphene to enhance the energy density of the flexible electrodes, as shown in Table 4 and 5.

3.1. CNTs/Conductive Polymer Composite Architectures

Because of their good electrical conductivity, pure SWCNTs-based electrodes are usually considered to be an electrode material that can provide a high power density.[7,15,128] However, their

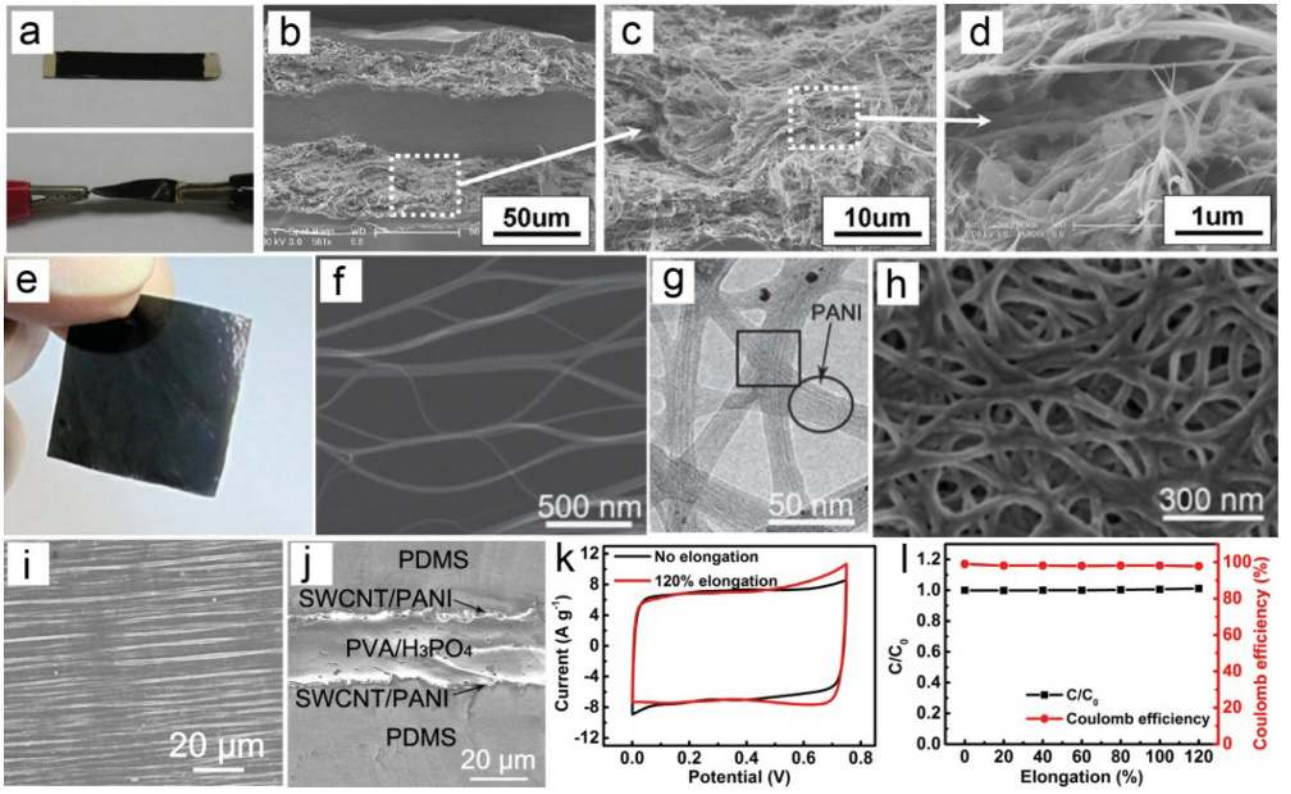

Figure 5. a) All-solid-state SC device using PANI coating CNT networks as electrodes at normal (top) and twisting (bottom) states. b–d) Cross-sectional SEM images of the ultrathin all-solid-state SC device based on PANI/CNT networks at different magnifications. Reproduced with permission.[29] Copyright 2010, American Chemical Society. e) Optical image of SWCNT/PANI composite film fabricated by in situ electrochemically polymerizing PANI in the directly grown SWCNT films. f) SEM image of SWCNT/PANI bundles with continuous network structure. g) TEM and h) SEM images of the SWCNT/PANI composite films. Reproduced with permission.[152] Copyright 2012, Royal Society of Chemistry. i) SEM images of buckled SWCNT/PANI film on PDMS substrate. j) The cross-section SEM image of the integrated SC based on buckled SWCNT/PANI film. k) CV curves of stretchable SC based on buckled SWCNT/PANI film at no and 120% strains. l) The variations of specific capacitance and coulomb efficiency of stretchable SC based on buckled SWCNT/PANI films at different strains. Reproduced with permission.[153] Copyright 2014, Springer.

specific surface area is, in general, low because SWCNTs often exist in the form of bundles. They therefore show a low energy density.[1,129] The porous structures and high conductivity of CNT films make them promising templates to load pseudo-capacitive materials. The specific capacitances of composite electrodes would be significantly enhanced by the synergetic effects of CNTs and conductive polymer.[26,130–141]

PANI is one of the most promising pseudo-capacitive materials due to its relatively high conductivity and low cost.[141–148] Using freestanding CNT films as templates, nanostructured PANI was deposited on the surface of CNTs to achieve CNT/PANI composite films.[132,136,149–151] For example, free-standing thin CNT/PANI composite films can be prepared by chemical polymerization of PANI on CNT networks. Using such CNT/PANI composite films as electrodes, ultrathin all-solid-state SC devices were developed by embedding two slightly separated CNT/PANI electrodes in the PVA/H_2SO_4 gel electrolyte (**Figure 5**a–d).[29] The thickness of such all-solid-state SC device is comparable to the case of a piece of A4-sized paper. In addition, free-standing SWCNT/PANI composite films were fabricated using an in situ process of electrochemically polymerizing PANI in the directly grown SWCNT films fabricated by FCCVD (Figure 5e).[152] Such SWCNT/PANI hybrid films show a "skeleton/skin" structure, in which the continuous SWCNT reticulate architecture and PANI layers acts as the skeleton and skin (Figure 5f–h), respectively. This unique continuous "skeleton/skin" structure provides composite films higher conductivity compared to the CNT/PANI hybrid films prepared by other methods. After spreading out SWCNT/PANI hybrid film onto the prestrained PDMS and releasing, the buckled SWCNT/PANI film was achieved on the PDMS substrate (Figure 5i). Using buckled SWCNT/PANI hybrid films and PVA/H_3PO_4 as electrodes and electrolyte, respectively, highly stretchable pseudo-SCs were fabricated (Figure 5j).[153] The resultant pseudo-SCs shows a stable performance at a 120% stretching strain, even after 1000 times repeated stretching. (Figure 5k,l). Apart from freestanding CNT films, the capacitances of substrate-supported CNT films can also be improved by depositing nanostructured PANI on the surface of CNTs.[154]

In addition to PANI, other conductive polymers, such as PPy and poly (3,4-ethylenedioxythiophene) (PEDOT) can also be used to enhance the energy density of CNT-based electrodes by the synergistic effects between CNTs and conductive polymer.[151,155–157] For example, free-standing PEDOT/poly(styrene sulfonate) (PSS)/SWCNT composite films that

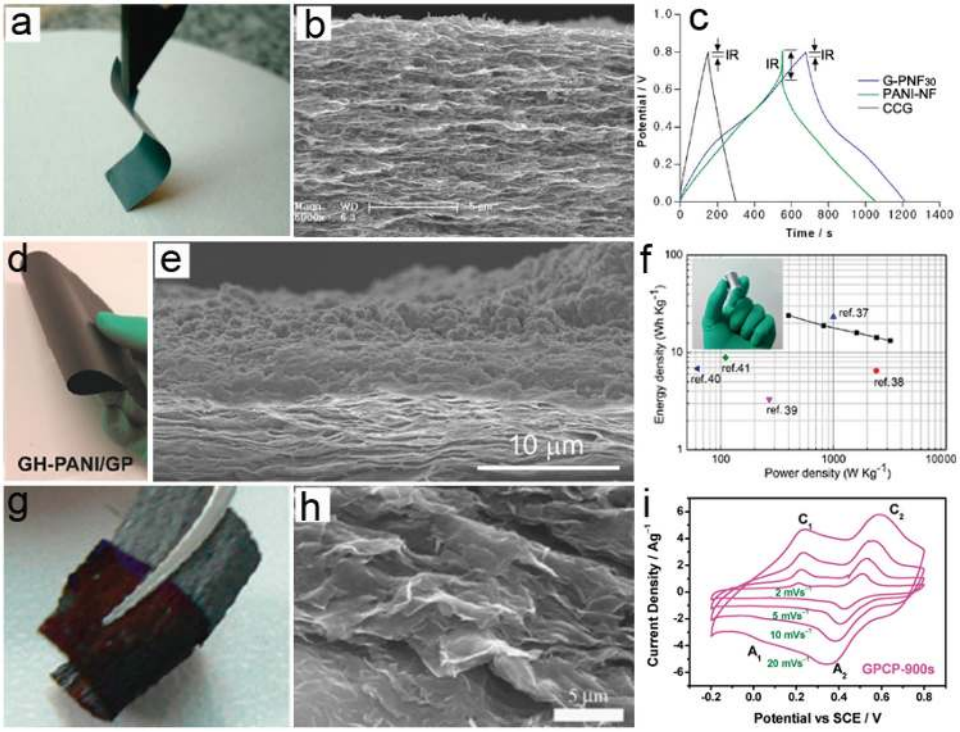

Figure 6. a) Optical and b) cross-section SEM images of rGO/PANI nanofiber film obtained by vacuum filtration. c) Charge/discharge curves of PANI, rGO and rGO/PANI films. Reproduced with permission.[147] Copyright 2010, American Chemical Society. d) Optical and e) SEM images of rGO hydrogel-PANI/graphene paper. f) Electrochemical performance of the SC device based on rGO hydrogel-PANI/graphene paper. Reproduced with permission.[166] Copyright 2014, American Chemical Society. g) Optical images of rGO/PANI composite paper fabricated by in situ electrochemical polymerization (bottom) and pure rGO paper (top). h) SEM image of rGO/PANI composite paper. i) CV curves of SC devices based on rGO/PANI composite paper at different scan rates. Reproduced with permission.[167] Copyright 2009, American Chemical Society.

can control the compositions of PEDOT/PSS were prepared by vacuum filtration.[155] SWCNTs dispersed in the polymer matrix increases the capacitance by 65% and displays excellent capacity retention after 1000 cycles.

In Section 2.1, we mentioned that the pure CNT fibers could not be directly used as fiber SC electrodes due to their compact structure. Although the performance of CNT fiber can be improved by inducing functional groups on the CNTs using a gamma irradiation treatment in the presence of air, the CNT fiber often serve as the substrate to deposit other active SC electrode materials with pseudo-capacitance.[158–163] For example, after depositing PANI nanowires on the surface of CNT fiber, two CNT/PANI composite fibers as parallel electrodes were twisted to produce wire-shaped micro-SCs based on gel electrolyte.[160] Similar to the addition of spacer into the compact graphene film to separate the aggregation of graphene sheets, if the the conductive polymer is added into the inner of the CNT fiber to form porous structure, the electrochemical performance of the CNT fiber would be enhanced. Therefore, PEDOT was first deposited on the surface of the aligned CNT sheets and then the biscrolled yarns were prepared by twisting PEDOT-coated MWNT sheets.[161] The gradient biscrolling in the yarns provides fast ion-transport yarn, where hundreds of layers of conducting-polymer-infiltrated CNT sheets are scrolled into an approximately 20 mm diameter yarn.

3.2. Graphene/Conductive Polymer Composite Architectures

The addition of a spacer, such as Au or carbon black NPs, can effectively prevent the restacking of rGO sheets in the films. Different from Au and carbon black NPs, the conductive polymer nanostructures not only prevent the restacking between rGO sheets in the films, but also enhance the energy density of rGO-based films due to the pseudo-capacitance from conductive polymer. For example, rGO/PANI-nanofiber films can be achieved using a vacuum filtration method, as shown **Figure 6**a,b.[147] The rGO/PANI-nanofiber film possess a conductivity of 5.5×10^2 S m^{-1}, which is much higher than the case of pure PANI-nanofiber film. The rGO/PANI-nanofiber film displays high performance in comparison with pure PANI and rGO films (Figure 6c). Combining electrostatic adsorption and vacuum filtration, highly ordered, layered poly(sodium 4-styrenesulfonate)-rGO/PANI composite papers can also be prepared by vacuum filtering of the as-prepared poly(sodium 4-styrenesulfonate), rGO, and PANI nanofibers mixed suspension, in which positively charged PANI nanofibers absorbed onto the negatively charged poly(sodium 4-styrenesulfonate) mediated rGO sheets.[164] In addition, flexible multilayered rGO/PANI composite films were fabricated by alternate layer-by-layer (LBL) deposition of positively charged PANI and negatively charged GO nanosheets on a substrate, followed by chemically reducing GO to rGO.[165] Based on a well-controlled

full inkjet printing method, a 3D rGO-PANI composite hydrogel can be fabricated on rGO paper, as shown in Figure 6d,e.[166] In such composite electrodes, 3D porous rGO hydrogel scaffold with nanostructured PANI significantly improves the electrical conductivity and energy density of the composite hydrogel (Figure 6f) and rGO paper endows composite electrode with excellent mechanical properties and high conductivity.

Porous rGO films can be directly used as template to deposit the conductive polymer nanomaterials by a variety of methods, such as electrochemical and chemical polymerization, because of their high surface area and high accessibility for the solution that was used to form conductive polymer nanomaterials.[167–171] For example, flexible rGO/PANI composite papers were fabricated by in situ electrochemical polymerization of PANI on rGO paper (Figure 6g,h).[167] These composite films show a good specific capacitance of 233 F g^{-1} (Figure 6i) and have a 58% enhancement compared to the rGO paper (147 F g^{-1}). The composite electrodes show an enhanced electronic conductivity due to the good contact between rGO sheets and excellent chemical stability during the charge/discharge process.

In addition to PANI, PPy can also be incorporated into graphene architectures to fabricate composite electrodes with high energy density. For instance, multilayered architectures consisting of rGO sheets and PPy nanowires have been successfully achieved by using liquid-air interface assembly and LBL assembly based on capillary force.[172] In such multilayered films, the PPy fibrous network leads to high ionic accessibility and aligned rGO sheets with high conductivity can act as current collectors.

3.3. Graphene/CNTs/Conductive Polymer Composite Architectures

During doping/dedoping processes of conductive polymers, the differential strain of polymer chains can be released by the synergistic effects from the flexibility of rGO sheets and the rigid properties of CNTs, resulting in excellent cyclic stability.[134,173] PPy/CNT composites can be well distributed between rGO sheets through flow-assembly to fabricate flexible hybrid films.[174] In such a multilayered architecture, the coaxial PPy/CNT nanocables are able to separate the rGO sheets and provide pseudo-capacitance to improve the energy density of electrodes. Because the intrinsic differential strain in PPy chains could be effective released by the synergistic effect from the flexible rGO sheet layer and the rigid CNT core, the specific capacitance of the rGO/PPy/CNT electrode only lost 5% of original capacity after 5000 cycles. Apart from PPy, PANI has also been successfully added into the graphene nanoribbon-CNT hybrid films, achieving a PANI-graphene nanoribbon-CNT composite film by in situ polymerization of aniline monomers on the surface of a graphene nanoribbon-CNT hybrid film.[175]

Nanocarbon-based materials often show good stability, but their capacitance is relatively low since not all their BET surface area can be electrochemically accessible. Accordingly, various conductive polymer nanostructure materials such as PANI, PPy, and PEDOT have been assembled into the nanocarbon architectures, forming flexible composite materials. They have high capacitance due to the synergetic effects of nanocarbon material and conductive polymer. However, in general, their power density is usually degraded compared to the pure nanocarbon-based electrodes, which is ascribed to the poor electrical conductivity of conductive polymer. Furthermore, the swelling and shrinkage of conductive polymers as SC electrodes will often degrade the cycling stability of carbon-based composite electrode materials. Therefore, two of the most critical aspects in fabricating nanocarbon/conductive polymer composite electrodes are to enhance their energy density without degrading their high power density and remain good cycling stability since these parameters is of great significance in the actual application of SCs. In addition, the intrinsic rigidity of conductive polymer often leads to poor flexibility, resulting in degraded flexibility of composite electrodes. Compared with CNT films, porous graphene architectures in general have larger surface area. Therefore, the loading of conductive polymers in porous graphene architectures is higher than the case of CNT films. However, the power density of CNT/conductive polymer composite films is higher in comparison to that of graphene/conductive polymer composite architectures due to the better conductivity of CNTs, as shown in Table 4.

4. Nanocarbon/Transition Metal Oxide Composite Architectures

Transition metal oxides are one of the best candidates for pseudo-capacitive SC electrode materials because they have high specific capacitance and very low resistance. Previous work shows that the energy density of SC electrodes can be effectively enhanced by using nanostructured transition metal oxides, such as MnO_2 and RuO_2, to provide pseudo-capacitance. The high surface area of rGO sheets and CNTs is able to serve as a promising support to deposit nanostructured transition metal oxides. Furthermore, because of the excellent conductivity of rGO and CNTs, the electrons in the reversible redox reaction of transition metal oxides can be easily transported through the rGO or CNT network, which result in improved power density of nanocarbon/transition metal oxide composite electrodes. In addition, the excellent mechanical properties of CNTs and rGO ensure that nanocarbon/transition metal oxide composite electrodes possess good flexibility.

4.1. CNT/Transition Metal Oxide Composite Architectures

Among transition metal oxides, hydrous manganese oxide had attracted most attention as a candidate for pseudo-SCs since the raw material is low-cost and manganese oxide is more environmentally friendly than other transition metal oxides. Using CNT films (**Figure 7**a,b) that pulled directly from a MWCNT array as the scaffold, MnO_x nanomaterials could be electrodeposited onto the surface of CNTs, obtaining flexible CNT/MnO_x composite films.[176] The morphology and microstructure of the CNT/MnO_x hybrid films can be well controlled by tuning electrodeposition time (Figure 7c–e). The specific capacitance and rate capability of such CNT/MnO_x composite electrodes depend on the size of MnO_x NPs on the CNT surface. The resultant CNT/MnO_x hybrid films show high specific

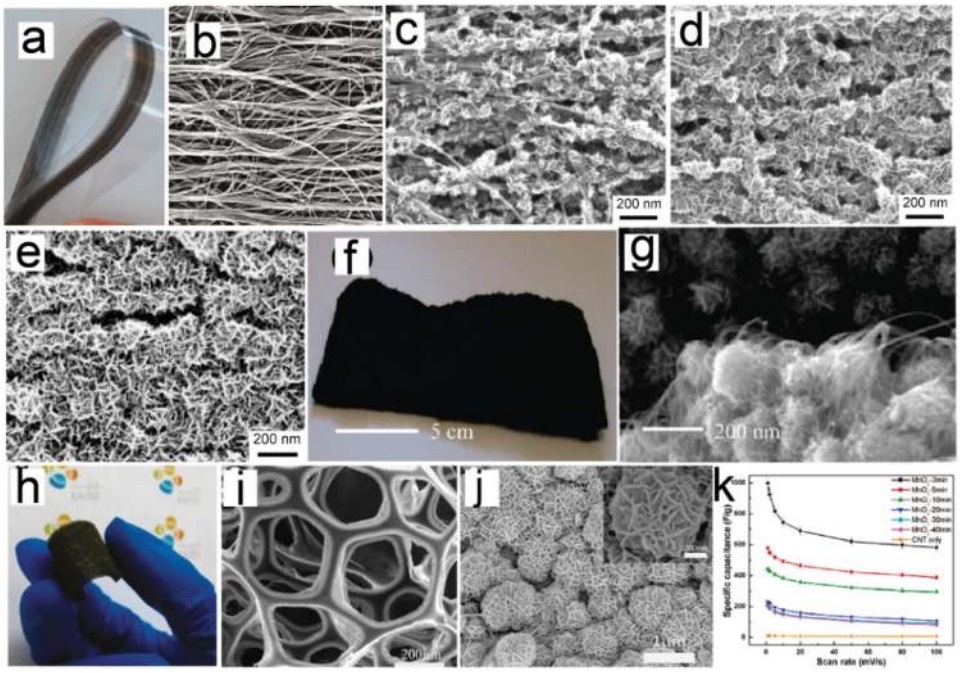

Figure 7. a) The CNT film pulled directly from CNT forest. SEM images of the MnO_x composites deposited for b) 0, c) 5, d)15, and e) 30 s. Reproduced with permission.[176] Copyright 2011, American Chemical Society. f) Optical and g) SEM images of MnO_2-coated SWNT/cotton composite. Reproduced with permission.[59] Copyright 2010, American Chemical Society. h) Optical and i,j) SEM images of a MnO_2-CNT-sponge composite. k) The specific capacitance of MnO_2-CNT-sponge composites with respect to the mass of MnO_2. Reproduced with permission.[178] Copyright 2011, American Chemical Society.

capacitance (1250 F g^{-1}), excellent charge/discharge rate capability, and good cyclic stability, which are ascribed to the synergistic effect between the MnO_x NPs and CNT films. Using other CNT structure as template, CNT/MnO_2 hybrid electrodes with flexibility can also be fabricated.[105,177]

As it is mentioned in Section 2.1, CNT can be coated onto the surface of textiles and paper to obtain SC electrodes with high flexibility. The porous structure of these CNT-coating textiles, sponges, and paper endow them with the ability to support transition metal oxide nanostructures to improve their performance.[59,178–180] For instance, highly conductive SWCNTs-coating cloth was achieved using a dipping and drying process based on a SWCNT suspension.[59] To enhance the specific capacitance of the SWCNT-coating cloth, MnO_2 was electrodeposited on the surface of SWCNTs, as shown in Figure 7f and g.[59] Although the mass loading of MnO_2 is remarkably increased in MnO_2/SWCNTs/cloth composite electrodes, SWCNTs still maintain good contact and provide pathway of transporting electrons. In addition, MnO_2 nanostructures can also be electrodeposited onto CNT-coating textile fibers or sponges to enhance the specific capacitance of electrodes (Figure 7h–k).[178,179]

Transition metal oxide nanowires have unique properties, such as high aspect ratio and short diffusion path length for ions, leading to large surface area and fast charge/discharge. Based on a solution of transition metal oxide nanowires, such as RuO_2, In_2O_3, and MnO_2, the transition metal oxide nanowires with a reasonable density can be coated onto the surface of SWCNT film that was fabricated by various methods.[181–183] For instance, thin SWCNT films can be printed on different flexible substrates and cloth fabrics by an off-the-shelf inkjet printer using SWCNT ink. The pattern geometry, location, thickness, and electrical conductivity can be well controlled by this method.[182] RuO_2 nanowires can then be coated on the surface of above the SWCNT films. Because of the addition of RuO_2, the SC based on SWCNT/RuO_2 composite film shows remarkably improved performance: specific capacitance of 138 F g^{-1}, power density of 96 kW kg^{-1}, and energy density of 18.8 Wh kg^{-1}. In this work, not all RuO_2 nanowires can contact SWCNTs, which is different from the case of CNT/MnO_2 composite films mentioned above. Therefore, the synergic effect of SWCNTs and RuO_2 nanowires may not work well. To further enhance the energy density of SC devices based on metal oxides, asymmetric SCs are often be designed.[184] The operation voltage of asymmetric SCs can be significantly increased by using two electrodes with different potential windows. Asymmetric SCs can be prepared using SWCNT/MnO_2 and SWCNT/In_2O_3 hybrid films as electrodes.[183] In the asymmetric SC, a MnO_2 nanowire/SWCNT composite film served as the positive electrode, while a In_2O_3 nanowire/SWCNT composite film acted as the negative electrode.

In addition to MnO_2 and In_2O_3, other transition metal oxides were also developed to enhance the energy density of the nanocarbon-based electrodes.[185,186] In general, vanadium oxides can provide high pseudo-capacitance but limited specific surface area and electrical conductivity. To overcome this problem, nanostructured vanadium oxide was deposited onto the surface of porous CNT electrodes via atomic layer deposition and the thicknesses of vanadium oxide layer can be well controlled.[185] The resultant composite films have controlled porosity, enhanced electrical conductivity, and cycle stability. In addition, freestanding mesoporous vanadium nitride nanowires/CNT

composite films were prepared using a simple vacuum filtering method. Such composite films effectively utilize the synergistic effects of the high electrochemical performance of vanadium nitride nanowires and the excellent conductivity and mechanical properties of the CNTs.[187] All-solid-state flexible SCs with high performance can be assembled based on such vanadium nitride nanowire/CNTs composite films and PVA/H_3PO_4 gel electrolyte.

4.2. Graphene/Transition Metal Oxide Composite Architectures

Because a variety of negatively charged oxygen containing functional groups are on the basal plane and the edge of GO sheet, GO sheets can be well dispersed in water or some organic solvents due to the repulsive interaction between oxygen containing functional groups.[80] This is different from the case of CNTs, especially SWCNTs, in which various surfactants usually disperse CNTs. As a result, GO sheet can directly act as a substrate to deposit transition metal oxide nanostructures. Subsequently, GO sheets with transition metal oxide nanostructures can be assembled into freestanding film. For example, GO/MnO_2 dispersion can be prepared by preparing MnO_2 NPs on the GO surfaces. By vacuum filtrating the GO/MnO_2 dispersion, flexible GO/MnO_2 hybrid papers would be successfully fabricated. After thermal reduction, the GO sheets in the composite film can be reduced to rGO, obtaining rGO/MnO_2 hybrid paper.[188,189] These rGO/MnO_2 hybrid papers can directly serve as flexible SC electrodes (**Figure 8**a).

Porous graphene films can be obtained by various methods, as mentioned in Section 2.2. Becasue of the appropriate porous structure (Figure 8b) and high mechanical properties, transition metal oxide nanomaterials can be directly fabricated on the surface of rGO in the films, achieving composite architectures.[190,191] For instance, porous rGO films are able to be achieved using a replicating and embossing technique in which polystyrene colloidal particles were used as sacrificial templates.[191] To improve the specific capacitance of such porous rGO films, nanostructured MnO_2 was deposited onto the surface of rGO sheets in the films, as shown in Figure 8c. The macroporous composite structure provides a large surface area and enhances the ionic transport in the electrode. Furthermore, asymmetric SC devices can be fabricated using pure rGO macroporous film and rGO/MnO_2 composite film as both electrodes of SCs. The resultant asymmetric SCs show an energy density of 44 Wh kg^{-1}, power density of 25 kW kg^{-1} (Figure 8d), and excellent cycle life. In addition, rGO foam obtained by assembling rGO onto the surface of Ni foam can also be used as support to deposit MnO_2 nanoparticles (Figure 8e).[192] After removing the Ni foam, flexible rGO/MnO_2 foam electrodes were achieved.

rGO nanosheets can be coated on the fiber surface of porous textiles by a solution-based coating technology. rGO-coating textiles are able to serve as a conductive scaffold to deposit MnO_2 NPs (Figure 8f–h).[193] Porous structure of textiles can increase the loading of SWCNTs and MnO_2 NPs and facilitate the diffusion of electrolytes into the composite textiles. Furthermore, the power density and cycle stability of rGO/MnO_2-coating textile can be further improved using a conductive wrapping method.[194] Because of the conductive wrapping of CNTs or conductive polymer on rGO/MnO_2 nanostructures, the specific capacitance of rGO/MnO_2 electrodes was significantly improved. In addition, rGO sheets and nanostructured MnO_2 can also be assembled onto the carbon fibers to form MnO_2/rGO/carbon fiber composite fiber electrodes. Using MnO_2/rGO/carbon fiber as the positive electrode and rGO/copper wire as negative electrode, asymmetric SC devices with excellent flexibility (Figure 8h) were prepared. The asymmetric

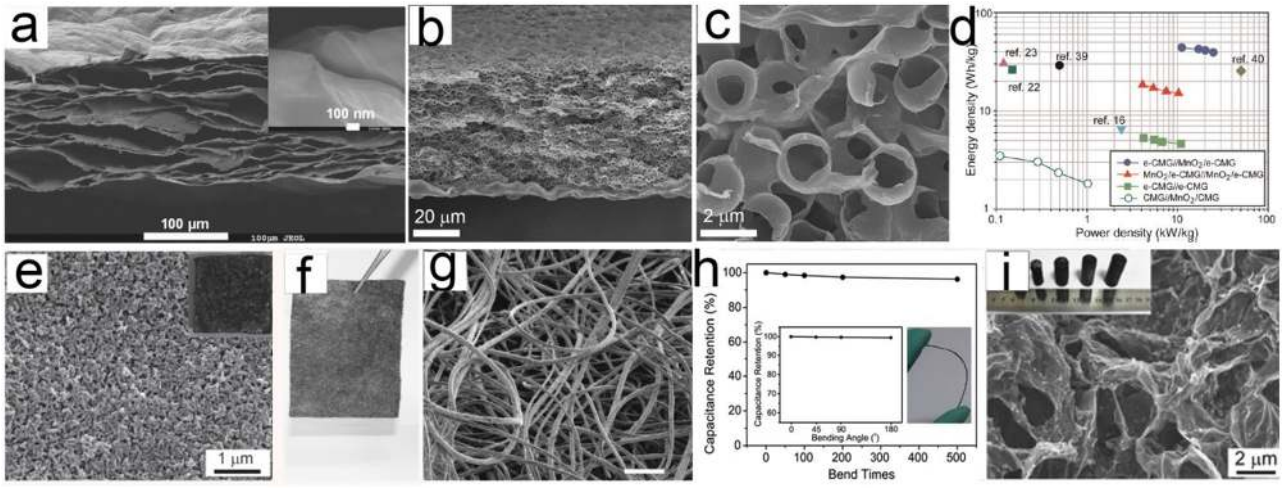

Figure 8. a) Cross sectional SEM image of rGO/MnO_2 paper. Reproduced with permission.[189] SEM images of b) the embossed rGO film and c) rGO/MnO_2 composite. d) The electrochemical performance of SCs based on the rGO/MnO_2 composite. Reproduced with permission.[191] Copyright 2012, American Chemical Society. e) SEM image of MnO_2 nanoparticles on the rGO foam. Reproduced with permission.[192] f) Optical and g) SEM images of graphene-coated conductive textile sheet, scale bar: 2 μm. Reproduced with permission.[194] Copyright 2011, American Chemical Society. h) Capacitance change of the asymmetric SC device based on rGO/MnO_2/carbon fiber and rGO hydrogel/copper wire electrodes at different bending states. Reproduced with permission.[195] i) The SEM image of rGO/TiO_2 obtained by a hydrothermal process. Reproduced with permission.[200] Copyright 2013, American Chemical Society.

fiber SCs were able to cycle reversibly in a voltage window of 0–1.6 V, displaying high areal and volumetric energy densities.[195] The asymmetric film SCs were also achieved based on graphene/MnO_2 composite films and they exhibit high energy density.[189,192,196,197]

Apart from MnO_2, other transition metal oxides also exhibit the capacity of enhancing the specific capacitance of graphene-based SC electrodes, as shown in Figure 8i.[198–200] For example, ZnO with tailoring nanostructures can easily grow on various substrates, especially on graphene films. The nanostructured ZnO often show pseudo-capacitance behavior. 3D vertical aligned ZnO nanorods that were sandwiched between rGO films can be prepared to serve as flexible SC electrodes.[198] ZnO nanorods in such composite electrodes are able to avoid the aggregation of rGO sheets to obtain porous structures.

4.3. Graphene/CNT/Transition Metal Oxide Composite Architectures

Because graphene has unique structural and electrical properties, it has been widely used as a scaffold for coating functional materials with ultrathin thickness. Interconnected network in CNT films can benefit electronic and ionic transport because of its excellent conductivity and porosity. Although MnO_2 can provide high pseudo-capacitance, its low conductivity will degrade the overall power density of SC devices. If the advantages of graphene, CNTs, and MnO_2 can be fully utilized, the composite electrodes based on them can achieve enhanced performance. For instance, conductive, highly flexible rGO/MnO_2/CNTs composite film electrodes were achieved by vacuum filtering a solution of CNT and rGO/MnO_2 composite. In such composite films, rGO sheets offer high surface area to grow MnO_2 NPs and CNTs enhance the electron conductance and mechanical reinforcement, thus allowing realization of the synergistic effects of rGO and CNTs. The synergistic effects from rGO, CNTs, and MnO_2 provide superior mechanical properties and outstanding electrochemical performance, which cannot be obtained using any of these components individually. The composite film can be rolled to rods with 0.5 mm diameter to fabricate compact high-performance SC devices, suggesting the significant potential as flexible SC electrodes. Based on LBL assembly, graphene layers were alternatively inserted between MWCNT films that were coated by V_2O_5 layers with 3 nm thickness, forming V_2O_5/MWCNT/graphene hybrid films.[201] The insertion of graphene can effectively avoid the agglomeration between the MWCNT films and increase the specific capacitance by 67% (about 2590 F g^{-1}). In addition, free-standing Co_3O_4/rGO/CNTs composite paper with high flexibility can be prepared by one-step hydrothermal process and they show a specific capacitance of 378 F g^{-1} with excellent electrochemical stability.[202]

In addition to the transition metal oxides, transition metal hydroxides and transition metal sulphides are also used as pseudo-capacitive materials.[12,203] The transition metal hydroxide, such as $Ni(OH)_2$, $Co(OH)_2$ and Co-Al hydroxide can be incorporated into the nanocarbon architectures for flexible SC electrodes.[204–212] The common transition metal sulfides used as pseudocapacitive electrodes are MoS_2, WS_2 VS_2 and $NiCo_2S_4$.[213–218] Furthermore, transition metal sulfides can also be added into nanocarbon architectures to serve as flexible SC electrodes.[214,219]

Because different transition metal oxides/ hydroxides have been successfully prepared in the graphene/CNTs composite architectures, asymmetric SCs can be obtained using these composite architectures as electrodes.[220–225] For example, the asymmetric SCs assembled by rGO/CNT/MnO_2 and rGO/CNT/PPy hybrid films are able to provide an output voltage of 1.6 V, and deliver high energy/power density (22.8 W h kg^{-1} at 860 W kg^{-1} and 2.7 kW kg^{-1} at 6.2 W h kg^{-1}).[223]

In general, nanocarbon/transition metal oxides architectures often display higher energy density than conventional carbon electrode materials and better electrochemical stability than nanocarbon/conductive polymers. However, compared to carbon materials and conductive polymers, the conductivity of transition metal oxides is lower. Therefore, the power density of the nanocarbon/transition metal oxide architectures is lower than the case of nanocarbon/conductive polymer composites. In addition, the frequently used liquid and gel electrolytes with acids cannot be used in the devices based on nanocarbon/transition metal oxide composite electrodes, as shown in Table 5, because acids in liquid and gel electrolytes will react with transition metal oxides. Therefore the solid state SC based on nanocarbon/transition metal oxide composite electrodes was rarely reported.

5. Summary and Perspectives

This article summarizes recent developments in the design and programmable assembly of flexible nanocarbons and their composite SC electrodes, including CNTs, graphene, CNT/graphene, CNTs/conductive polymer, graphene/conductive polymer, CNTs/graphene/conductive polymer, CNTs/transition metal oxides, graphene/transition metal oxides, and CNTs/graphene/transition metal oxides. Compared with conventional supercapacitor electrodes based on carbon, conductive polymers, and/or metal oxides, these flexible nanocarbon-based electrodes are freestanding or substrate-supported, avoiding the use of metal current collector, conductive additives or binders, due to the high conductivity and good mechanical properties of CNTs and graphene. Furthermore, they usually have programmable and tunable features, such as controllable porous structure and components. The high conductivity of pure CNTs and graphene electrodes endows them with high power density, but the aggregation of CNTs and graphene in the corresponding film electrodes leads to low energy density. To enhance their energy density, two types of active electrochemical materials, namely conductive polymer and transition metal oxides, were introduced into the nanocarbon architectures. The resulting composite architectures have improved energy density and retain their good flexibility by combining the high pseudocapacitance of conductive polymer and transition metal oxides with high conductivity and good mechanical properties of CNTs and graphene, as shown in **Table 6**. Additionally, we have highlighted the assembly of flexible SC devices based on these nanocarbon-based architectures and compare their performance.

Currently, a great amount of progress has been made in the fabrication of flexible nanocarbon-based electrodes and the

Table 6. Comparison between flexible SC electrodes based on CNTs and graphene.

	Flexiblility	Electrolyte	Energy density [Wh kg^{-1}]	Power density [kWkg^{-1}]	Cycle life
CNT	high	aqueous	–	8	high
		organic	47	200	high
		solid state	6–49	23–32	high
CNT-conductive polymer	mediun	acid or neutral	15–33	0.1–10	low
		organic	131	62.5	low
		solid state	0.5–7.1	0.3–2	low
CNT-transition metal oxide	mediun	neutral	5–135	1–96	low
Graphene	mediun	aqueous	15–50	1–414	high
		organic	26–153	2.4–500	high
		solid state	1–10 mWh cm^{-3}	0.01–20 W cm^{-3}	high
Graphene-conductive polymer	mediun	acid or neutral	15–33	1–10	low
		solid state	24–36	<1	low
Graphene –transition metal oxide	mediun	neutral	2–44	25–110	low

design of flexible SC devices, however, much work remains to be done. For instance, various flexible CNTs- and graphene-based SC electrodes have been achieved using different methods, such as solution-based coating, vacuum filtration, and printing techniques, however, fully utilizing the specific surface area, conductivity, and mechanical properties of graphene and CNTs in flexible nanocarbon electrodes is still a challenge. The properties of flexible nanocarbon architecture electrodes greatly depend on their orientation and connection of CNTs or graphene. Thus further efforts are needed for the design of the ordered and controllable microstructures and programmable assembly. In addition, the BET surface area of reported graphene films with porous structures is much lower than the case of single graphene sheets because of the aggregation of graphene sheets. Controlling the assembly of graphene sheets into macroscopic porous films can effectively avoid the restacking of graphene sheets to make the surface of graphene sheets fully accessible. Furthermore, the overall capacitance of flexible SC devices based on nanocarbon-based electrodes is too small to meet the demand of practical applications because of the limited mass and area of flexible SC electrodes. Flexible SC devices with both high flexibility and capacitance should be considered for practical applications.

In addition to single phase flexible nanocarbon electrodes that only consist of CNTs or graphene, nanocarbon-based composite electrodes including pseudocapacitive materials can significantly extend the scope of flexible nanocarbon electrodes. However, the power densities and cycling stability of reported composite electrodes are often remarkably degraded due to the poor conductivity and the structure that is easily damaged during the redox process of pseudocapacitive additives. For composite electrodes, another problem is that their flexibility is decreased due to the intrinsic rigidity of the pseudocapacitive additives. To overcome these problems, new strategies that programmably control the morphology, distribution, orientation, and mass loading of pseudocapacitive additives in composite architectures are desired to realize the synergistic effect and the optimization between nanocarbon materials and pseudocapacitive additives.

The configuration of SC devices can also affect the performance and flexibility of SCs. The flexible SC devices are frequently fabricated by arranging two electrodes and a separator in a sandwich form, followed by filling electrolyte and sealed with two plastic slices. Liquid electrolytes are often used in this kind of devices, however, their flexibility is medium because the sealing position is easily cracked under the bending state and the intrinsic flexibility of plastic is limited. Solid SCs can be achieved based on gel electrolytes. These solid SCs are highly flexible, and even foldable and stretchable, and avoid the leakage of electrolyte. However, the electrochemical performance of solid SCs is lower compared with their counterpart based on liquid electrolyte due to the slow ionic conductivity of gel electrolytes (Table 6). Thus high-performance gel electrolytes should be explored. Because a variety of flexible electronic devices with different functions have been fabricated, flexible SC devices with various configurations have to be further designed to match and power these electronic devices, and even integrate the flexible SCs with these electronic devices into fully flexible devices.[226]

Although various nanocarbon-based architectures have been prepared and different types of flexible SCs were designed and assembled using these nanocarbon-based architectures as electrodes, the measurement methods for the electrochemical performance and flexibility of nanocarbon-based electrodes and flexible SCs are not well standardized.[227] Therefore, it is difficult to accurately evaluate and compare the true performance of nanocarbon-based architectures and corresponding devices reported in the literature because they were tested in different systems. For example, the specific capacitances of the electrode materials for a three-electrode system are in general double those of the two-electrode system. In addition, the performance of the SC devices depends on the electrolyte, separator, and device configuration, which are different in different systems. Furthermore, the size and thickness of nanocarbon-based architectures vary widely in different devices, which also influences the measured results. Various techniques and configurations will yield remarkably varying results. Therefore,

reliable measurements for SC devices should be developed. For flexible SCs, it is required that the performance of the SC devices be evaluated under different bending states. Therefore, in the future, unified testing methods for flexible SCs at different states should be considered.

At different bending states, the physical and electrochemical properties of carbon-based electrodes and the distribution of electrolyte in electrodes may be varied in comparison with the case at no bending state. However, using current in situ technology, it is is difficult to detect the electrode and electrolyte under bending conditions. Thus, it is urgent to simplify the configuration of the supercapacitor and develop in situ technology to realize the direct detection of the electrode and electrolyte in different states.

Acknowledgements

This work was supported by the Singapore National Research Foundation (CREATE Programme of Nanomaterials for Energy and Water Management), the National Basic Research Program of China (Grant No. 2012CB932302), the MOE (IRT13R30) of China, the National Natural Science Foundation of China (51172271, 51372269 and 90921012), the "Strategic Priority Research Program" of the Chinese Academy of Sciences (XDA09040202), and the Fund of Beijing Municipal Education Commission (Grant No. YB20108000101).

Received: April 6, 2015
Revised: June 4, 2015
Published online:

[1] L. L. Zhang, X. S. Zhao, *Chem. Soc. Rev.* **2009**, *38*, 2520.
[2] Y. Zhang, H. Feng, X. B. Wu, L. Z. Wang, A. Q. Zhang, T. C. Xia, H. C. Dong, X. F. Li, L. S. Zhang, *Int. J. Hydrogen Energy* **2009**, *34*, 4889.
[3] P. Simon, Y. Gogotsi, *Nat. Mater.* **2008**, *7*, 845.
[4] M. Winter, R. J. Brodd, *Chem. Rev.* **2004**, *104*, 4245.
[5] Y. G. Wang, Y. Y. Xia, *Adv. Mater.* **2013**, *25*, 5336.
[6] J. Wang, L. Shen, B. Ding, P. Nie, H. Deng, H. Dou, X. Zhang, *RSC Adv.* **2014**, *4*, 7538.
[7] M. Kaempgen, C. K. Chan, J. Ma, Y. Cui, G. Gruner, *Nano Lett.* **2009**, *9*, 1872.
[8] G. Zhou, F. Li, H.-M. Cheng, *Energy Environ. Sci.* **2014**, *7*, 1307.
[9] Z. Y. Cao, B. Q. Wei, *Energy Environ. Sci.* **2013**, *6*, 3183.
[10] L. Nyholm, G. Nystrom, A. Mihranyan, M. Stromme, *Adv. Mater.* **2011**, *23*, 3751.
[11] K. Jost, D. Stenger, C. R. Perez, J. K. McDonough, K. Lian, Y. Gogotsi, G. Dion, *Energy Environ. Sci.* **2013**, *6*, 2698.
[12] X. Peng, L. Peng, C. Wu, Y. Xie, *Chem. Soc. Rev.* **2014**, *43*, 3303.
[13] J. Yan, Q. Wang, T. Wei, Z. Fan, *Adv. Energy Mater.* **2014**, *4*, 1300816.
[14] X. Wang, X. Lu, B. Liu, D. Chen, Y. Tong, G. Shen, *Adv. Mater.* **2014**, *26*, 4763.
[15] Z. Q. Niu, W. Y. Zhou, J. Chen, G. X. Feng, H. Li, W. J. Ma, J. Z. Li, H. B. Dong, Y. Ren, D. Zhao, S. S. Xie, *Energy Environ. Sci.* **2011**, *4*, 1440.
[16] W. Y. Zhou, X. D. Bai, E. G. Wang, S. S. Xie, *Adv. Mater.* **2009**, *21*, 4565.
[17] Z. Q. Niu, W. J. Ma, H. B. Dong, J. Z. Li, W. Y. Zhou, *Chin. Phys. B* **2011**, *20*, 028101.
[18] W. Y. Zhou, W. J. Ma, Z. Q. Niu, L. Song, S. S. Xie, *Chin. Sci. Bull.* **2012**, *57*, 205.
[19] L. Song, L. Ci, L. Lv, Z. P. Zhou, X. Q. Yan, D. F. Liu, H. J. Yuan, Y. Gao, J. X. Wang, L. F. Liu, X. W. Zhao, Z. X. Zhang, X. Y. Dou, W. Y. Zhou, G. Wang, C. Y. Wang, S. S. Xie, *Adv. Mater.* **2004**, *16*, 1529.
[20] W. J. Ma, L. Song, R. Yang, T. H. Zhang, Y. C. Zhao, L. F. Sun, Y. Ren, D. F. Liu, L. F. Liu, J. Shen, Z. X. Zhang, Y. J. Xiang, W. Y. Zhou, S. S. Xie, *Nano Lett.* **2007**, *7*, 2307.
[21] L. Q. Liu, W. J. Ma, Z. Zhang, *Small* **2011**, *7*, 1504.
[22] C. Li, G. Q. Shi, *Nanoscale* **2012**, *4*, 5549.
[23] L. Liu, Z. Niu, L. Zhang, X. Chen, *Small* **2014**, *10*, 2200.
[24] Z. Q. Niu, L. Liu, L. Zhang, X. Chen, *Small* **2014**, *10*, 3434.
[25] T. Chen, L. Dai, *J. Mater. Chem. A* **2014**, *2*, 10756.
[26] L. Y. Yuan, X. H. Lu, X. Xiao, T. Zhai, J. J. Dai, F. C. Zhang, B. Hu, X. Wang, L. Gong, J. Chen, C. G. Hu, Y. X. Tong, J. Zhou, Z. L. Wang, *ACS Nano* **2012**, *6*, 656.
[27] F. H. Meng, Y. Ding, *Adv. Mater.* **2011**, *23*, 4098.
[28] Z. S. Wu, A. Winter, L. Chen, Y. Sun, A. Turchanin, X. L. Feng, K. Müllen, *Adv. Mater.* **2012**, *24*, 5130.
[29] C. Z. Meng, C. H. Liu, L. Z. Chen, C. H. Hu, S. S. Fan, *Nano Lett.* **2010**, *10*, 4025.
[30] B. G. Choi, J. Hong, W. H. Hong, P. T. Hammond, H. Park, *ACS Nano* **2011**, *5*, 7205.
[31] C. Shi, Q. Zhao, H. Li, Z.-M. Liao, D. Yu, *Nano Energy* **2014**, *6*, 82.
[32] B. Liu, B. Liu, X. Wang, D. Chen, Z. Fan, G. Shen, *Nano Energy* **2014**, *10*, 99.
[33] D. Wei, S. J. Wakeham, T. W. Ng, M. J. Thwaites, H. Brown, P. Beecher, *Electrochem. Commun.* **2009**, *11*, 2285.
[34] Y. J. Kang, H. Chung, C. H. Han, W. Kim, *Nanotechnology* **2012**, *23*, 289501.
[35] Y. Huang, J. J. Liang, Y. S. Chen, *Small* **2012**, *8*, 1805.
[36] L. M. Dai, D. W. Chang, J. B. Baek, W. Lu, *Small* **2012**, *8*, 1130.
[37] L. Li, Z. Wu, S. Yuan, X.-B. Zhang, *Energy Environ. Sci.* **2014**, *7*, 2101.
[38] X. Lu, M. Yu, G. Wang, Y. Tong, Y. Li, *Energy Environ. Sci.* **2014**, *7*, 2160.
[39] A. S. Arico, P. Bruce, B. Scrosati, J. M. Tarascon, W. Van Schalkwijk, *Nat. Mater.* **2005**, *4*, 366.
[40] R. H. Baughman, A. A. Zakhidov, W. A. de Heer, *Science* **2002**, *297*, 787.
[41] Y. Q. Sun, Q. O. Wu, G. Q. Shi, *Energy Environ. Sci.* **2011**, *4*, 1113.
[42] Z. C. Wu, Z. H. Chen, X. Du, J. M. Logan, J. Sippel, M. Nikolou, K. Kamaras, J. R. Reynolds, D. B. Tanner, A. F. Hebard, A. G. Rinzler, *Science* **2004**, *305*, 1273.
[43] D. H. Zhang, K. Ryu, X. L. Liu, E. Polikarpov, J. Ly, M. E. Tompson, C. W. Zhou, *Nano Lett.* **2006**, *6*, 1880.
[44] L. Cooper, H. Amano, M. Hiraide, S. Houkyou, I. Y. Jang, Y. J. Kim, H. Muramatsu, J. H. Kim, T. Hayashi, Y. A. Kim, M. Endo, M. S. Dresselhaus, *Appl. Phys. Lett.* **2009**, *95*, 233104.
[45] C. M. Niu, E. K. Sichel, R. Hoch, D. Moy, H. Tennent, *Appl. Phys. Lett.* **1997**, *70*, 1480.
[46] W. J. Ma, L. Q. Liu, Z. Zhang, R. Yang, G. Liu, T. H. Zhang, X. F. An, X. S. Yi, Y. Ren, Z. Q. Niu, J. Z. Li, H. B. Dong, W. Y. Zhou, P. M. Ajayan, S. S. Xie, *Nano Lett.* **2009**, *9*, 2855.
[47] Z. Q. Niu, W. Y. Zhou, J. Chen, G. X. Feng, H. Li, Y. S. Hu, W. J. Ma, H. B. Dong, J. Z. Li, S. S. Xie, *Small* **2013**, *9*, 518.
[48] L. Cai, J. Z. Li, P. S. Luan, H. B. Dong, D. Zhao, Q. Zhang, X. Zhang, M. Tu, Q. S. Zeng, W. Y. Zhou, S. S. Xie, *Adv. Funct. Mater.* **2012**, *22*, 5238.
[49] L. Cai, L. Song, P. Luan, Q. Zhang, N. Zhang, Q. Gao, D. Zhao, X. Zhang, M. Tu, F. Yang, W. Zhou, Q. Fan, J. Luo, W. Zhou, P. M. Ajayan, S. Xie, *Sci. Rep.* **2013**, *3*, 3048.
[50] C. J. Yu, C. Masarapu, J. P. Rong, B. Q. Wei, H. Q. Jiang, *Adv. Mater.* **2009**, *21*, 4793.
[51] Z. Q. Niu, H. B. Dong, B. W. Zhu, J. Z. Li, H. H. Hng, W. Y. Zhou, X. D. Chen, S. S. Xie, *Adv. Mater.* **2013**, *25*, 1058.

[52] G. Y. Zheng, Y. Cui, E. Karabulut, L. Wagberg, H. L. Zhu, L. B. Hu, *MRS Bull.* **2013**, *38*, 320.
[53] A. C. Siegel, S. T. Phillips, M. D. Dickey, N. Lu, Z. Suo, G. M. Whitesides, *Adv. Funct. Mater.* **2010**, *20*, 28.
[54] A. D. Mazzeo, W. B. Kalb, L. Chan, M. G. Killian, J. F. Bloch, B. A. Mazzeo, G. M. Whitesides, *Adv. Mater.* **2012**, *24*, 2850.
[55] L. Y. Yuan, B. Yao, B. Hu, K. F. Huo, W. Chen, J. Zhou, *Energy Environ. Sci.* **2013**, *6*, 470.
[56] W. J. Hyun, O. O. Park, B. D. Chin, *Adv. Mater.* **2013**, *25*, 4729.
[57] Z. J. Shi, G. O. Phillips, G. Yang, *Nanoscale* **2013**, *5*, 3194.
[58] L. B. Hu, J. W. Choi, Y. Yang, S. Jeong, F. La Mantia, L. F. Cui, Y. Cui, *Proc. Natl Acad. Sci. USA* **2009**, *106*, 21490.
[59] L. B. Hu, M. Pasta, F. La Mantia, L. F. Cui, S. Jeong, H. D. Deshazer, J. W. Choi, S. M. Han, Y. Cui, *Nano Lett.* **2010**, *10*, 708.
[60] S. Hu, R. Rajamani, X. Yu, *Appl. Phys. Lett.* **2012**, *100*, 104103.
[61] B. Hsia, J. Marschewski, S. Wang, J. B. In, C. Carraro, D. Poulikakos, C. P. Grigoropoulos, R. Maboudian, *Nanotechnology* **2014**, *25*.
[62] A. L. M. Reddy, M. M. Shaijumon, S. R. Gowda, P. M. Ajayan, *J. Phys. Chem. C* **2010**, *114*, 658.
[63] V. L. Pushparaj, M. M. Shaijumon, A. Kumar, S. Murugesan, L. Ci, R. Vajtai, R. J. Linhardt, O. Nalamasu, P. M. Ajayan, *Proc. Natl Acad. Sci. USA* **2007**, *104*, 13574.
[64] P. X. Li, C. Y. Kong, Y. Y. Shang, E. Z. Shi, Y. T. Yu, W. Z. Qian, F. Wei, J. Q. Wei, K. L. Wang, H. W. Zhu, A. Y. Cao, D. H. Wu, *Nanoscale* **2013**, *5*, 8472.
[65] W. J. Ma, L. Q. Liu, R. Yang, T. H. Zhang, Z. Zhang, L. Song, Y. Ren, J. Shen, Z. Q. Niu, W. Y. Zhou, S. S. Xie, *Adv. Mater.* **2009**, *21*, 603.
[66] K. Jiang, Q. Li, S. Fan, *Nature* **2002**, *419*, 801.
[67] M. Zhang, K. R. Atkinson, R. H. Baughman, *Science* **2004**, *306*, 1358.
[68] X. B. Zhang, K. L. Jiang, C. Teng, P. Liu, L. Zhang, J. Kong, T. H. Zhang, Q. Q. Li, S. S. Fan, *Adv. Mater.* **2006**, *18*, 1505.
[69] Q. Meng, H. Wu, Y. Meng, K. Xie, Z. Wei, Z. Guo, *Adv. Mater.* **2014**, *26*, 4100.
[70] Z. Gui, H. L. Zhu, E. Gillette, X. G. Han, G. W. Rubloff, L. B. Hu, S. B. Lee, *ACS Nano* **2013**, *7*, 6037.
[71] V. T. Le, H. Kim, A. Ghosh, J. Kim, J. Chang, Q. A. Vu, D. T. Pham, J. H. Lee, S. W. Kim, Y. H. Lee, *ACS Nano* **2013**, *7*, 5940.
[72] Z. B. Yang, J. Deng, X. L. Chen, J. Ren, H. S. Peng, *Angew. Chem. Int. Ed.* **2013**, *52*, 13453.
[73] M. D. Stoller, S. J. Park, Y. W. Zhu, J. H. An, R. S. Ruoff, *Nano Lett.* **2008**, *8*, 3498.
[74] C. Lee, X. D. Wei, J. W. Kysar, J. Hone, *Science* **2008**, *321*, 385.
[75] Y. W. Zhu, S. Murali, W. W. Cai, X. S. Li, J. W. Suk, J. R. Potts, R. S. Ruoff, *Adv. Mater.* **2010**, *22*, 5226.
[76] S. Y. Yin, Z. Q. Niu, X. D. Chen, *Small* **2012**, *8*, 2458.
[77] X. Cui, C. Z. Zhang, R. Hao, Y. L. Hou, *Nanoscale* **2011**, *3*, 2118.
[78] D. A. Dikin, S. Stankovich, E. J. Zimney, R. D. Piner, G. H. B. Dommett, G. Evmenenko, S. T. Nguyen, R. S. Ruoff, *Nature* **2007**, *448*, 457.
[79] D. Chen, L. H. Tang, J. H. Li, *Chem. Soc. Rev.* **2010**, *39*, 3157.
[80] D. R. Dreyer, S. Park, C. W. Bielawski, R. S. Ruoff, *Chem. Soc. Rev.* **2010**, *39*, 228.
[81] K. R. Paton, E. Varrla, C. Backes, R. J. Smith, U. Khan, A. O'Neill, C. Boland, M. Lotya, O. M. Istrate, P. King, T. Higgins, S. Barwich, P. May, P. Puczkarski, I. Ahmed, M. Moebius, H. Pettersson, E. Long, J. Coelho, S. E. O'Brien, E. K. McGuire, B. M. Sanchez, G. S. Duesberg, N. McEvoy, T. J. Pennycook, C. Downing, A. Crossley, V. Nicolosi, J. N. Coleman, *Nat. Mater.* **2014**, *13*, 624.
[82] D. Li, M. B. Muller, S. Gilje, R. B. Kaner, G. G. Wallace, *Nat. Nanotechnol.* **2008**, *3*, 101.
[83] X. W. Yang, J. W. Zhu, L. Qiu, D. Li, *Adv. Mater.* **2011**, *23*, 2833.
[84] L. L. Zhang, X. Zhao, M. D. Stoller, Y. W. Zhu, H. X. Ji, S. Murali, Y. P. Wu, S. Perales, B. Clevenger, R. S. Ruoff, *Nano Lett.* **2012**, *12*, 1806.
[85] Z. X. Tai, X. B. Yan, Q. J. Xue, *J. Power Sources* **2012**, *213*, 350.
[86] A. P. Yu, I. Roes, A. Davies, Z. W. Chen, *Appl. Phys. Lett.* **2010**, *96*, 253105.
[87] G. K. Wang, X. Sun, F. Y. Lu, H. T. Sun, M. P. Yu, W. L. Jiang, C. S. Liu, J. Lian, *Small* **2012**, *8*, 452.
[88] C. M. Chen, Q. Zhang, C. H. Huang, X. C. Zhao, B. S. Zhang, Q. Q. Kong, M. Z. Wang, Y. G. Yang, R. Cai, D. S. Su, *Chem. Commun.* **2012**, *48*, 7149.
[89] Z. Q. Niu, J. J. Du, X. B. Cao, Y. H. Sun, W. Y. Zhou, H. H. Hng, J. Ma, X. D. Chen, S. S. Xie, *Small* **2012**, *8*, 3201.
[90] S. Biswas, L. T. Drzal, *ACS Appl. Mater. Interfaces* **2010**, *2*, 2293.
[91] Z. Q. Niu, J. Chen, H. H. Hng, J. Ma, X. D. Chen, *Adv. Mater.* **2012**, *24*, 4144.
[92] Y. Xu, Z. Lin, X. Zhong, X. Huang, N. O. Weiss, Y. Huang, X. Duan, *Nat. Commun.* **2014**, *5*, 4554.
[93] M. F. El-Kady, V. Strong, S. Dubin, R. B. Kaner, *Science* **2012**, *335*, 1326.
[94] M. F. El-Kady, R. B. Kaner, *Nat. Commun.* **2013**, *4*, 1475.
[95] W. Gao, N. Singh, L. Song, Z. Liu, A. L. M. Reddy, L. J. Ci, R. Vajtai, Q. Zhang, B. Q. Wei, P. M. Ajayan, *Nat. Nanotechnol.* **2011**, *6*, 496.
[96] Z. Q. Niu, L. Zhang, L. L. Liu, B. W. Zhu, H. B. Dong, X. D. Chen, *Adv. Mater.* **2013**, *25*, 4035.
[97] W. W. Liu, Y. Q. Feng, X. B. Yan, J. T. Chen, Q. J. Xue, *Adv. Funct. Mater.* **2013**, *23*, 4111.
[98] S.-K. Kim, H.-J. Koo, A. Lee, P. V. Braun, *Adv. Mater.* **2014**, *26*, 5108.
[99] J. T. Li, F. Ye, S. Vaziri, M. Muhammed, M. C. Lemme, M. Ostling, *Adv. Mater.* **2013**, *25*, 3985.
[100] Z. S. Wu, K. Parvez, X. L. Feng, K. Mullen, *Nat. Commun.* **2013**, *4*, 3487.
[101] Z. S. Wu, K. Parvez, X. L. Feng, K. Mullen, *J. Mater. Chem. A* **2014**, *2*, 8288.
[102] Z.-S. Wu, K. Parvez, A. Winter, H. Vieker, X. Liu, S. Han, A. Turchanin, X. Feng, K. Müllen, *Adv. Mater.* **2014**, *26*, 4552.
[103] J. J. Yoo, K. Balakrishnan, J. S. Huang, V. Meunier, B. G. Sumpter, A. Srivastava, M. Conway, A. L. M. Reddy, J. Yu, R. Vajtai, P. M. Ajayan, *Nano Lett.* **2011**, *11*, 1423.
[104] Y. R. Kang, Y. L. Li, F. Hou, Y. Y. Wen, D. Su, *Nanoscale* **2012**, *4*, 3248.
[105] Z. Weng, Y. Su, D. W. Wang, F. Li, J. H. Du, H. M. Cheng, *Adv. Energy Mater.* **2011**, *1*, 917.
[106] L. L. Liu, Z. Q. Niu, L. Zhang, W. Y. Zhou, X. D. Chen, S. S. Xie, *Adv. Mater.* **2014**, *26*, 4855.
[107] W. W. Liu, X. B. Yan, J. W. Lang, C. Peng, Q. J. Xue, *J. Mater. Chem.* **2012**, *22*, 17245.
[108] Z. L. Dong, C. C. Jiang, H. H. Cheng, Y. Zhao, G. Q. Shi, L. Jiang, L. T. Qu, *Adv. Mater.* **2012**, *24*, 1856.
[109] X. M. Li, T. S. Zhao, K. L. Wang, Y. Yang, J. Q. Wei, F. Y. Kang, D. H. Wu, H. W. Zhu, *Langmuir* **2011**, *27*, 12164.
[110] E. Y. Jang, J. Carretero-Gonzalez, A. Choi, W. J. Kim, M. E. Kozlov, T. Kim, T. J. Kang, S. J. Baek, D. W. Kim, Y. W. Park, R. H. Baughman, Y. H. Kim, *Nanotechnology* **2012**, *23*, 235601.
[111] Z. Xu, C. Gao, *Nat. Commun.* **2011**, *2*, 571.
[112] Y. N. Meng, Y. Zhao, C. G. Hu, H. H. Cheng, Y. Hu, Z. P. Zhang, G. Q. Shi, L. T. Qu, *Adv. Mater.* **2013**, *25*, 2326.
[113] Z. Xu, Z. Liu, H. Y. Sun, C. Gao, *Adv. Mater.* **2013**, *25*, 3249.
[114] Z. Xu, H. Y. Sun, X. L. Zhao, C. Gao, *Adv. Mater.* **2013**, *25*, 188.
[115] X. Zang, Q. Chen, P. Li, Y. He, X. Li, M. Zhu, X. Li, K. Wang, M. Zhong, D. Wu, H. Zhu, *Small* **2014**, *10*, 2583.
[116] G. Sun, J. Liu, X. Zhang, X. Wang, H. Li, Y. Yu, W. Huang, H. Zhang, P. Chen, *Angew. Chem. Int. Ed.* **2014**, *53*, 12576.

[117] L. W. Peng, Y. Y. Feng, P. Lv, D. Lei, Y. T. Shen, Y. Li, W. Feng, *J. Phys. Chem. C* **2012**, *116*, 4970.
[118] X. J. Lu, H. Dou, B. Gao, C. Z. Yuan, S. D. Yang, L. Hao, L. F. Shen, X. G. Zhang, *Electrochim. Acta* **2011**, *56*, 5115.
[119] Y. F. Li, Y. Z. Liu, Y. G. Yang, M. Z. Wang, Y. F. Wen, *Appl. Phys. A* **2012**, *108*, 701.
[120] L. Qiu, X. Yang, X. Gou, W. Yang, Z.-F. Ma, G. G. Wallace, D. Li, *Chem.-Eur. J.* **2010**, *16*, 10653.
[121] D. S. Yu, L. M. Dai, *J. Phys. Chem. Lett.* **2010**, *1*, 467.
[122] J. Lin, C. G. Zhang, Z. Yan, Y. Zhu, Z. W. Peng, R. H. Hauge, D. Natelson, J. M. Tour, *Nano Lett.* **2013**, *13*, 72.
[123] M. Beidaghi, C. L. Wang, *Adv. Funct. Mater.* **2012**, *22*, 4501.
[124] F. S. Wen, C. X. Hao, J. Y. Xiang, L. M. Wang, H. Hou, Z. B. Su, W. T. Hu, Z. Y. Liu, *Carbon* **2014**, *75*, 236.
[125] D. S. Yu, K. Goh, H. Wang, L. Wei, W. C. Jiang, Q. Zhang, L. M. Dai, Y. Chen, *Nat. Nanotechnol.* **2014**, *9*, 555.
[126] D. Yu, K. Goh, Q. Zhang, L. Wei, H. Wang, W. Jiang, Y. Chen, *Adv. Mater.* **2014**, *26*, 6790.
[127] J. I. Talpone, P. F. Puleston, J. J. More, R. Grino, M. G. Cendoya, *Int. J. Hydrogen Energy* **2012**, *37*, 10346.
[128] A. Izadi-Najafabadi, T. Yamada, D. N. Futaba, M. Yudasaka, H. Takagi, H. Hatori, S. Iijima, K. Hata, *ACS Nano* **2011**, *5*, 811.
[129] V. V. N. Obreja, *Physica E* **2008**, *40*, 2596.
[130] M. N. Hyder, S. W. Lee, F. C. Cebeci, D. J. Schmidt, Y. Shao-Horn, P. T. Hammond, *ACS Nano* **2011**, *5*, 8552.
[131] R. V. Salvatierra, M. M. Oliveira, A. J. G. Zarbin, *Chem. Mater.* **2010**, *22*, 5222.
[132] C. Z. Meng, C. H. Liu, S. S. Fan, *Electrochem. Commun.* **2009**, *11*, 186.
[133] A. A. Mikhaylova, E. K. Tusseeva, N. A. Mayorova, A. Y. Rychagov, Y. M. Volfkovich, A. V. Krestinin, O. A. Khazova, *Electrochim. Acta* **2011**, *56*, 3656.
[134] J. Yan, T. Wei, Z. J. Fan, W. Z. Qian, M. L. Zhang, X. D. Shen, F. Wei, *J. Power Sources* **2010**, *195*, 3041.
[135] T. Wang, A. Kiebele, J. Ma, S. Mhaisalkar, G. Gruner, *J. Electrochem. Soc.* **2011**, *158*, A1.
[136] J. Ge, G. H. Cheng, L. W. Chen, *Nanoscale* **2011**, *3*, 3084.
[137] J. L. Liu, J. Sun, L. Gao, *Nanoscale* **2011**, *3*, 3616.
[138] J. E. Huang, X. H. Li, J. C. Xu, H. L. Li, *Carbon* **2003**, *41*, 2731.
[139] T. M. Wu, Y. W. Lin, C. S. Liao, *Carbon* **2005**, *43*, 734.
[140] J. A. Lee, M. K. Shin, S. H. Kim, S. J. Kim, G. M. Spinks, G. G. Wallace, R. Ovalle-Robles, M. D. Lima, M. E. Kozlov, R. H. Baughman, *ACS Nano* **2012**, *6*, 327.
[141] Q. Liu, O. Nayfeh, M. H. Nayfeh, S. T. Yau, *Nano Energy* **2013**, *2*, 133.
[142] C. Peng, S. W. Zhang, D. Jewell, G. Z. Chen, *Prog. Nat. Sci.* **2008**, *18*, 777.
[143] Y. Z. Liao, C. Zhang, Y. Zhang, V. Strong, J. S. Tang, X. G. Li, K. Kalantar-zadeh, E. M. V. Hoek, K. L. Wang, R. B. Kaner, *Nano Lett.* **2011**, *11*, 954.
[144] H. L. Wang, Q. L. Hao, X. J. Yang, L. D. Lu, X. Wang, *Nanoscale* **2010**, *2*, 2164.
[145] X. B. Yan, Z. X. Tai, J. T. Chen, Q. J. Xue, *Nanoscale* **2011**, *3*, 212.
[146] H. S. Fan, H. Wang, N. Zhao, X. L. Zhang, J. Xu, *J. Mater. Chem.* **2012**, *22*, 2774.
[147] Q. Wu, Y. X. Xu, Z. Y. Yao, A. R. Liu, G. Q. Shi, *ACS Nano* **2010**, *4*, 1963.
[148] Q. A. Liu, M. H. Nayfeh, S. T. Yau, *J. Power Sources* **2010**, *195*, 7480.
[149] S. Q. He, J. Q. Wei, F. M. Guo, R. Q. Xu, C. Li, X. Cui, H. W. Zhu, K. L. Wang, D. H. Wu, *J. Mater. Chem. A* **2014**, *2*, 5898.
[150] T. Chen, H. S. Peng, M. Durstock, L. M. Dai, *Sci. Rep.* **2014**, *4*, 3612.
[151] H. J. Lin, L. Li, J. Ren, Z. B. Cai, L. B. Qiu, Z. B. Yang, H. S. Peng, *Sci. Rep.* **2013**, *3*, 1353.
[152] Z. Q. Niu, P. S. Luan, Q. Shao, H. B. Dong, J. Z. Li, J. Chen, D. Zhao, L. Cai, W. Y. Zhou, X. D. Chen, S. S. Xie, *Energy Environ. Sci.* **2012**, *5*, 8726.
[153] N. Zhang, P. S. Luan, W. Y. zhou, Q. Zhang, L. Cai, X. Zhang, S. S. Xie, *Nano Res.* **2014**, *7*, 1680.
[154] K. Wang, P. Zhao, X. M. Zhou, H. P. Wu, Z. X. Wei, *J. Mater. Chem.* **2011**, *21*, 16373.
[155] D. Antiohos, G. Folkes, P. Sherrell, S. Ashraf, G. G. Wallace, P. Aitchison, A. T. Harris, J. Chen, A. I. Minett, *J. Mater. Chem.* **2011**, *21*, 15987.
[156] P. X. Li, E. Z. Shi, Y. B. Yang, Y. Y. Shang, Q. Y. Peng, S. T. Wu, J. Q. Wei, K. L. Wang, H. W. Zhu, Q. Yuan, A. Y. Cao, D. H. Wu, *Nano Res.* **2014**, *7*, 209.
[157] P. X. Li, Y. B. Yang, E. Z. Shi, Q. C. Shen, Y. Y. Shang, S. T. Wu, J. Q. Wei, K. L. Wang, H. W. Zhu, Q. Yuan, A. Y. Cao, D. H. Wu, *ACS Appl. Mater. Interfaces* **2014**, *6*, 5228.
[158] F. H. Su, M. H. Miao, H. T. Niu, Z. X. Wei, *ACS Appl. Mater. Interfaces* **2014**, *6*, 2552.
[159] K. Wang, Q. H. Meng, Y. J. Zhang, Z. X. Wei, M. H. Miao, *Adv. Mater.* **2013**, *25*, 1494.
[160] J. Ren, L. Li, C. Chen, X. L. Chen, Z. B. Cai, L. B. Qiu, Y. G. Wang, X. R. Zhu, H. S. Peng, *Adv. Mater.* **2013**, *25*, 1155.
[161] J. A. Lee, M. K. Shin, S. H. Kim, H. U. Cho, G. M. Spinks, G. G. Wallace, M. D. Lima, X. Lepro, M. E. Kozlov, R. H. Baughman, S. J. Kim, *Nat. Commun.* **2013**, *4*, 1970.
[162] Q. Meng, K. Wang, W. Guo, J. Fang, Z. Wei, X. She, *Small* **2014**, *10*, 3187.
[163] X. Chen, H. Lin, J. Deng, Y. Zhang, X. Sun, P. Chen, X. Fang, Z. Zhang, G. Guan, H. Peng, *Adv. Mater.* **2014**, *26*, 8126.
[164] S. Liu, X. H. Liu, Z. P. Li, S. R. Yang, J. Q. Wang, *New J. Chem.* **2011**, *35*, 369.
[165] T. Lee, T. Yun, B. Park, B. Sharma, H. K. Song, B. S. Kim, *J. Mater. Chem.* **2012**, *22*, 21092.
[166] K. Chi, Z. Zhang, J. Xi, Y. Huang, F. Xiao, S. Wang, Y. Liu, *ACS Appl. Mater. Interfaces* **2014**, *6*, 16312.
[167] D. W. Wang, F. Li, J. P. Zhao, W. C. Ren, Z. G. Chen, J. Tan, Z. S. Wu, I. Gentle, G. Q. Lu, H. M. Cheng, *ACS Nano* **2009**, *3*, 1745.
[168] H. P. Cong, X. C. Ren, P. Wang, S. H. Yu, *Energy Environ. Sci.* **2013**, *6*, 1185.
[169] A. Davies, P. Audette, B. Farrow, F. Hassan, Z. W. Chen, J. Y. Choi, A. P. Yu, *J. Phys. Chem. C* **2011**, *115*, 17612.
[170] Y. Xie, Y. Liu, Y. Zhao, Y. H. Tsang, S. P. Lau, H. Huang, Y. Chai, *J. Mater. Chem. A* **2014**, *2*, 9142.
[171] F. Xiao, S. X. Yang, Z. Y. Zhang, H. F. Liu, J. W. Xiao, L. Wan, J. Luo, S. Wang, Y. Q. Liu, *Sci. Rep.* **2015**, *5*, 9359.
[172] S. Biswas, L. T. Drzal, *Chem. Mater.* **2010**, *22*, 5667.
[173] K. S. Kim, S. J. Park, *Electrochim. Acta* **2011**, *56*, 1629.
[174] X. J. Lu, H. Dou, C. Z. Yuan, S. D. Yang, L. Hao, F. Zhang, L. F. Shen, L. J. Zhang, X. G. Zhang, *J. Power Sources* **2012**, *197*, 319.
[175] M. K. Liu, Y. E. Miao, C. Zhang, W. W. Tjiu, Z. B. Yang, H. S. Peng, T. X. Liu, *Nanoscale* **2013**, *5*, 7312.
[176] J. H. Kim, K. H. Lee, L. J. Overzet, G. S. Lee, *Nano Lett.* **2011**, *11*, 2611.
[177] P. Lv, P. Zhang, Y. Y. Feng, Y. Li, W. Feng, *Electrochim. Acta* **2012**, *78*, 515.
[178] L. B. Hu, W. Chen, X. Xie, N. A. Liu, Y. Yang, H. Wu, Y. Yao, M. Pasta, H. N. Alshareef, Y. Cui, *ACS Nano* **2011**, *5*, 8904.
[179] W. Chen, R. B. Rakhi, L. B. Hu, X. Xie, Y. Cui, H. N. Alshareef, *Nano Lett.* **2011**, *11*, 5165.
[180] Y. J. Kang, B. Kim, H. Chung, W. Kim, *Synth. Met.* **2010**, *160*, 2510.
[181] P. C. Chen, G. Shen, S. Sukcharoenchoke, C. Zhou, *Appl. Phys. Lett.* **2009**, *94*, 233104.
[182] P. C. Chen, H. T. Chen, J. Qiu, C. W. Zhou, *Nano Res.* **2010**, *3*, 594.

[183] P. C. Chen, G. Z. Shen, Y. Shi, H. T. Chen, C. W. Zhou, *ACS Nano* **2010**, *4*, 4403.
[184] J. Wang, L. Shen, P. Nie, X. Yun, Y. Xu, H. Dou, X. Zhang, *J. Mater. Chem. A* **2015**, *3*, 2853.
[185] S. Boukhalfa, K. Evanoff, G. Yushin, *Energy Environ. Sci.* **2012**, *5*, 6872.
[186] C. J. Chien, S. S. Deora, P. C. Chang, D. D. Li, J. G. Lu, *IEEE Trans. Nanotechnol.* **2011**, *10*, 706.
[187] X. Xiao, X. Peng, H. Y. Jin, T. Q. Li, C. C. Zhang, B. Gao, B. Hu, K. F. Huo, J. Zhou, *Adv. Mater.* **2013**, *25*, 5091.
[188] Z. P. Li, Y. J. Mi, X. H. Liu, S. Liu, S. R. Yang, J. Q. Wang, *J. Mater. Chem.* **2011**, *21*, 14706.
[189] A. Sumboja, C. Y. Foo, X. Wang, P. S. Lee, *Adv. Mater.* **2013**, *25*, 2809.
[190] Y. He, W. Chen, X. Li, Z. Zhang, J. Fu, C. Zhao, E. Xie, *ACS Nano* **2013**, *7*, 174.
[191] B. G. Choi, M. Yang, W. H. Hong, J. W. Choi, Y. S. Huh, *ACS Nano* **2012**, *6*, 4020.
[192] Z. Zhang, F. Xiao, L. Qian, J. Xiao, S. Wang, Y. Liu, *Adv. Energy Mater.* **2014**, *4*, 1400064.
[193] G. H. Yu, L. B. Hu, M. Vosgueritchian, H. L. Wang, X. Xie, J. R. McDonough, X. Cui, Y. Cui, Z. N. Bao, *Nano Lett.* **2011**, *11*, 2905.
[194] G. H. Yu, L. B. Hu, N. A. Liu, H. L. Wang, M. Vosgueritchian, Y. Yang, Y. Cui, Z. N. Bao, *Nano Lett.* **2011**, *11*, 4438.
[195] Z. Zhang, F. Xiao, S. Wang, *J. Mater. Chem. A* **2015**.
[196] Z. Wang, Z. Zhu, J. Qiu, S. Yang, *J. Mater. Chem. C* **2014**, *2*, 1331.
[197] Y. Shao, H. Wang, Q. Zhang, Y. Li, *J. Mater. Chem. C* **2013**, *1*, 1245.
[198] G. L. Guo, L. Huang, Q. H. Chang, L. C. Ji, Y. Liu, Y. Q. Xie, W. Z. Shi, N. Q. Jia, *Appl. Phys. Lett.* **2011**, *99*, 083111.
[199] K. Gopalsamy, Z. Xu, B. Zheng, T. Huang, L. Kou, X. Zhao, C. Gao, *Nanoscale* **2014**, *6*, 8595.
[200] Z. Zhang, F. Xiao, Y. Guo, S. Wang, Y. Liu, *ACS Appl. Mater. Interfaces* **2013**, *5*, 2227.
[201] I. Shakir, Z. Ali, J. Bae, J. Park, D. J. Kang, *Nanoscale* **2014**, *6*, 4125.
[202] C. Z. Yuan, L. Yang, L. R. Hou, J. Y. Li, Y. X. Sun, X. G. Zhang, L. F. Shen, X. J. Lu, S. L. Xiong, X. W. Lou, *Adv. Funct. Mater.* **2012**, *22*, 2560.
[203] G. Wang, L. Zhang, J. Zhang, *Chem. Soc. Rev.* **2012**, *41*, 797.
[204] C. Hao, F. Wen, J. Xiang, L. Wang, H. Hou, Z. Su, W. Hu, Z. Liu, *Adv. Funct. Mater.* **2014**, *24*, 6700.
[205] X. Dong, Z. Guo, Y. Song, M. Hou, J. Wang, Y. Wang, Y. Xia, *Adv. Funct. Mater.* **2014**, *24*, 3405.
[206] Y. Zhou, F. Hou, Z.-P. Wan, Y.-L. Tang, D.-M. Yang, S. Zhao, R. Peng, *ECS Solid State Lett.* **2014**, *3*, M1.
[207] J. Zhao, J. Chen, S. Xu, M. Shao, Q. Zhang, F. Wei, J. Ma, M. Wei, D. G. Evans, X. Duan, *Adv. Funct. Mater.* **2014**, *24*, 2938.
[208] Y. Ma, W. Chen, P. Zhang, F. Teng, J. Zhou, X. Pan, E. Xie, *RSC Adv.* **2014**, *4*, 47609.
[209] W. Lan, Y. Sun, Y. Chen, J. Wang, G. Tang, W. Dou, Q. Su, E. Xie, *RSC Adv.* **2015**, *5*, 20878.
[210] J. Yang, C. Yu, X. Fan, J. Qiu, *Adv. Energy Mater.* **2014**, *4*.
[211] X. Dong, L. Wang, D. Wang, C. Li, J. Jin, *Langmuir* **2012**, *28*, 293.
[212] X. Y. Dong, L. Wang, D. Wang, C. Li, J. Jin, *Langmuir* **2012**, *28*, 293.
[213] H. Tang, J. Wang, H. Yin, H. Zhao, D. Wang, Z. Tang, *Adv. Mater.* **2015**, *27*, 1117.
[214] S. Patil, A. Harle, S. Sathaye, K. Patil, *CrystEngComm* **2014**, *16*, 10845.
[215] K.-J. Huang, L. Wang, Y.-J. Liu, H.-B. Wang, Y.-M. Liu, L.-L. Wang, *Electrochim. Acta* **2013**, *109*, 587.
[216] L. Cao, S. Yang, W. Gao, Z. Liu, Y. Gong, L. Ma, G. Shi, S. Lei, Y. Zhang, S. Zhang, R. Vajtai, P. M. Ajayan, *Small* **2013**, *9*, 2905.
[217] M. Acerce, D. Voiry, M. Chhowalla, *Nat. Nanotechnol.* **2015**, *10*, 313.
[218] L. Shen, J. Wang, G. Xu, H. Li, H. Dou, X. Zhang, *Adv. Energy Mater.* **2015**, *5*, 1400977.
[219] Y. Li, K. Ye, K. Cheng, J. Yin, D. Cao, G. Wang, *J. Power Sources* **2015**, *274*, 943.
[220] Y. Cheng, H. Zhang, S. Lu, C. V. Varanasiad, J. Liu, *Nanoscale* **2013**, *5*, 1067.
[221] Z. Zhang, F. Xiao, L. Qian, J. Xiao, S. Wang, Y. Liu, *Adv. Energy Mater.* **2014**, *4*.
[222] G. Sun, X. Zhang, R. Lin, J. Yang, H. Zhang, P. Chen, *Angew. Chem. Int. Ed.* **2015**, *54*, 4651.
[223] J. Liu, L. Zhang, H. B. Wu, J. Lin, Z. Shen, X. W. Lou, *Energy Environ. Sci.* **2014**, *7*, 3709.
[224] Y. Jin, H. Chen, M. Chen, N. Liu, Q. Li, *ACS Appl. Mater. Interfaces* **2013**, *5*, 3408.
[225] H. Gao, F. Xiao, C. B. Ching, H. Duan, *ACS Appl. Mater. Interfaces* **2012**, *4*, 7020.
[226] B. Liu, B. Liu, X. Wang, X. Wu, W. Zhao, Z. Xu, D. Chen, G. Shen, *Adv. Mater.* **2014**, *26*, 4999.
[227] Y. Gogotsi, P. Simon, *Science* **2011**, *334*, 917.
[228] Y. W. Cheng, S. T. Lu, H. B. Zhang, C. V. Varanasi, J. Liu, *Nano Lett.* **2012**, *12*, 4206.